EXPERIMENTAL DETERMINATION OF THE FEASIBILITY OF WASTE HEAT RECOVERY IN DATA CENTERS USING EJECTOR BASED REFRIGERATION

A Thesis
Presented to
The Academic Faculty

by

Joshua Glenn Sharp

In Partial Fulfillment
of the Requirements for the Degree
Master of Science in the
School of Mechanical Engineering

Georgia Institute of Technology

August 2011

EXPERIMENTAL DETERMINATION OF THE FEASIBILITY OF WASTE HEAT RECOVERY IN DATA CENTERS USING EJECTOR BASED REFRIGERATION

Approved by:

Dr. Yogendra Joshi, Advisor
School of Mechanical Engineering
Georgia Institute of Technology

Dr. S. Mostafa Ghiaasiaan
School of Mechanical Engineering
Georgia Institute of Technology

Dr. Sheldon Jeter
School of Mechanical Engineering
Georgia Institute of Technology

Dr. Pramod Kumar
School of Mechanical Engineering
Georgia Institute of Technology

Date Approved: April 21, 2011

ACKNOWLEDGEMENTS

First, I would like to thank my advisor, Dr. Yogendra Joshi, for all of his expertise and direction throughout the research process. His dedication to the success of my research and his patience have aided me considerably as I prepared this thesis. I would also like to thank my committee members Dr. Mostafa Ghiaasiaan and Dr. Sheldon Jeter for their flexibility, support, expertise and interest in my success. I would like to especially thank Dr. Pramod Kumar for his daily suggestions and criticisms that helped to influence my experience based education.

Lastly, I would like to thank the support staff and students in the Microelectronics Thermal Laboratory. They provided their own unique perspective to the issues I experienced. I would especially like to thank Carter Dietz, Andrew Mcnamara, and Vivek Sahu for their assistance using the lab equipment in the Microelectronics Thermal Laboratory.

TABLE OF CONTENTS

LIST OF TABLES

LIST OF FIGURES

LIST OF SYMBOLS

ρ	density
ν	specific volume
A	area
$\dot{m}$	mass flow rate
P	pressure
Q	heat transfer
s	entropy per unit mass
T	temperature
V	velocity
W	work
w	entrainment ratio

Subscripts

1,2,3	different states of the system

SUMMARY

The purpose of this thesis is to experimentally determine the feasibility of an ejector based, waste heat recovery driven refrigeration system applied to the data center environment in order to reduce operational cooling costs. A comprehensive literature review is detailed to determine the current state of the ejector refrigeration research and assess the initial direction of this thesis. A simplified model was created to perform preliminary performance estimations and system sizing before constructing an experimental system apparatus to evaluate the model predictions. The pressures and temperatures used in the model and instituted in the experimental system are based on the maximum temperatures typically observed in computing servers (50-75°C). Precision controlled heaters are used to simulate the computer server heat, and R245fa is used as the working fluid. Performance results ranged from 0.06 to 0.13.

1. INTRODUCTION

In 2007, the Environmental Protection Agency reported to the U.S. Congress that data centers consumed 61 billion kilowatt-hours of electricity, which is roughly 1.5% of the total energy used in the United States, and that current projections indicate that data center energy use could nearly double in five years [1]. At the same time, improvements in information technology have caused the power density in data centers to increase substantially from a design point of about 1 kW/m^2 (100 W/ft^2) a decade ago, to up to 13.5 kW/m^2 (1250 W/ft^2) today. The monumental cooling infrastructure demanded by the increased power density of state-of-the-art computing racks is forcing many data centers into obsolescence. Combined with the volatility of energy prices, the cost of providing the essential service of server storage in a traditional data center is expected to increase dramatically in the coming years. Consequently, the data center industry must make significant efforts to contain the rapidly increasing costs associated with their daily operations, and to prepare for the swelling wave of new technologies that demand cooling above the limits of existing systems [2]. Additionally, current data center power density trends indicate that most data center facilities, many of which were build 6-10 years ago, will be unable to provide adequate cooling for new high power computer clusters, which dissipate between 20 and 40 kW per rack. Since a large number of data center buildings were designed for loads of 4-8 kW per rack, they will either need to be refit or demolished to accommodate the new wave of power dense server racks unless an alternate, more efficient cooling method can be developed. [3].

1.1 Quantifying Data Center Energy Efficiency

Before going any further, it is important to understand the industry metrics that are commonly used to provide historic perspective, benchmarks, and future expectations for data center efficiency. A popular metric used to describe the effective allocation of power in a data center is the Power Usage Effectiveness, or PUE. By definition, the PUE is the power used by the IT equipment (servers, data storage, networking hardware, etc.) plus the power used by the cooling equipment (server fans, computer room air conditioning unit fans, chiller compressor, etc.) divided by the power used by the IT equipment. From this definition, it is clear that as cooling efficiency improves, the PUE approaches one. A recent study has determined that most legacy data centers operate with a PUE of approximately 1.7 to 2.0. Recently constructed facilities that have incorporated alternate cooling methods in order to reduce power consumption have reported PUE of 1.2 [4]. The largest gains from alternative cooling techniques and improvements in energy efficiency will be had by data centers operating at a larger PUE.

1.2 Common Alternate Cooling Methods

Various products and cooling schemes have been demonstrated to ensure that existing data centers can economically handle the recent surge in rack power density. Though not all of the alternate cooling methods can be applied generally, many have reportedly reduced the cost of operation of existing data centers. Among the more commonly employed techniques impacting data center PUE are rear door heat exchangers, direct liquid cooled processors, ice storage, and waste heat recovery.

1.2.1 Rear Door Heat Exchangers

One of the inefficiencies inherent in the conventional data center design is the centralized computer room air conditioning units, or CRAC units. In this particular configuration, the hot air exhaust from server racks is collected and redirected to a few CRAC units, which cycle the hot

air over cooling coils via high powered fans. The cooled air is then returned to the room, either by utilizing an under floor plenum, or an overhead distribution system, as shown in Figure 1.

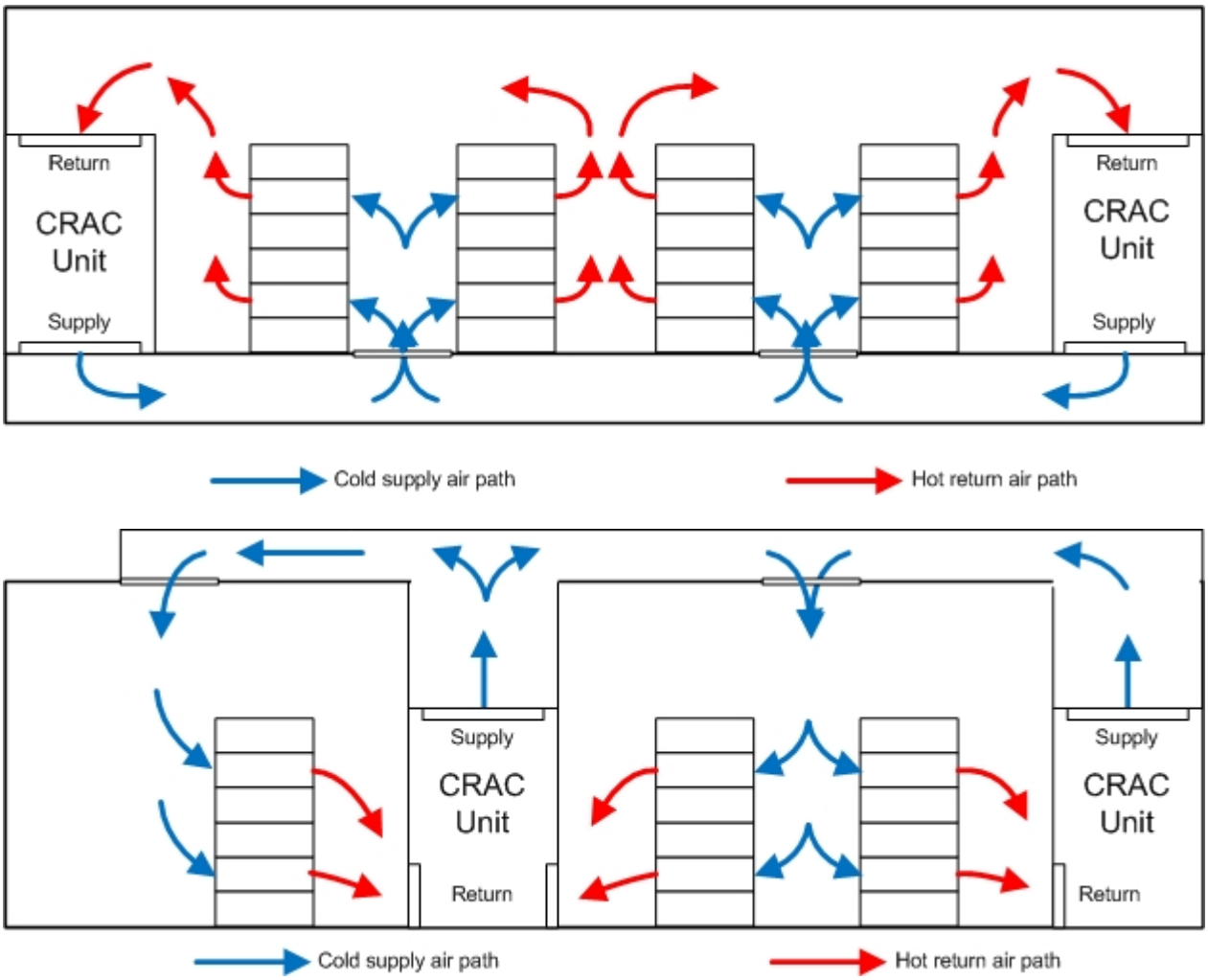

Figure 1. Under Floor Plenum (top) and Overhead Distribution (bottom)

The problem inherent in these two designs can be clearly understood and has been extensively documented through academic and industry studies on the subject. Among the more influential cooling inefficiency factors are recirculation, short circuiting, and wide swings in server load, either due to data center rack density concentrations or heat load variation. The rear door heat exchanger attempts to counteract these cooling concerns by essentially relocating the cooling coils of the CRAC unit to the exhaust side rack door and using the server fans to provide

the necessary air flow over the cooling coils instead of a large CRAC unit fan, severely reducing the requisite number of CRAC units [5]. According to the manufacturer, this could result in total energy savings of up to 90%, an increase in rack density (rack/sqft), and overall operational costs reduction of up to 50% [6]. The water distribution scheme is shown in Figure 2.

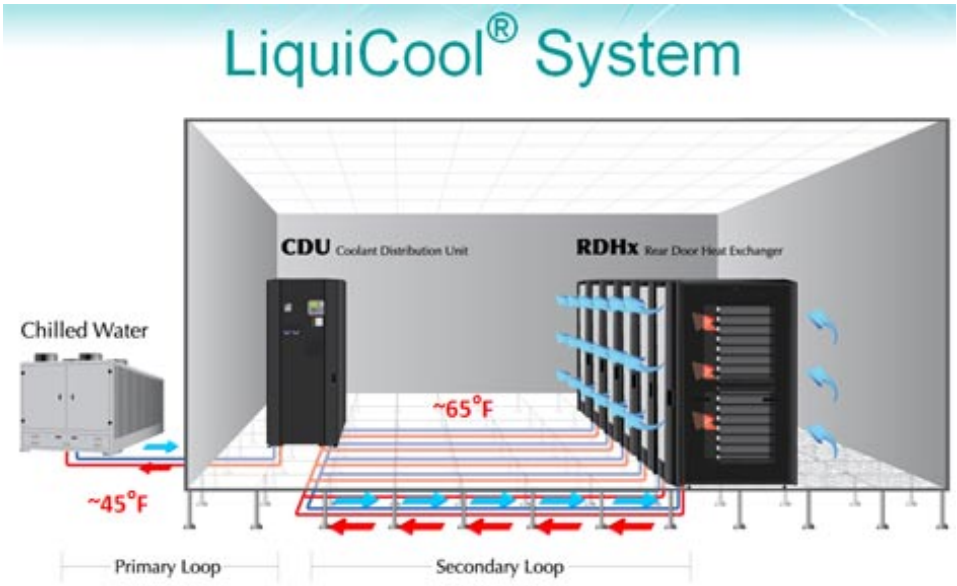

Figure 2. Rear Door Heat Exchanger Water Distribution Scheme (Courtesy of CoolCentric)

1.2.2 Liquid Cooled Processors

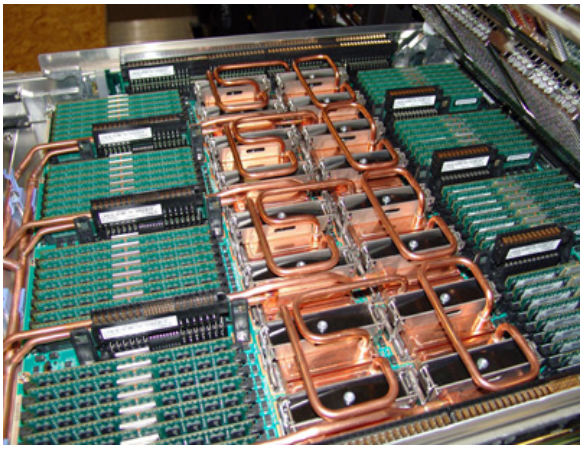

Figure 3. IBM Liquid Cooled Processors (Courtesy of IBM)

Even when utilizing a cooling solution like the rear door heat exchanger, emerging extremely high power racks that dissipate up to 60 kW would still require additional or even more sophisticated cooling techniques. In response, IBM has developed a hybrid cooling system for some of their most advanced computing racks. The hybrid system consists of an elaborate distribution system providing chilled water to the processors, while forced air convection is used to cool the remaining components, coupled with a rear door heat exchanger to reduce the load on the computer room air conditioning units [7]. Results from their development provide insight into some of the benefits of providing site specific liquid cooling instead of general area cooling that traditional methods supply. Cooling infrastructure reduction, hot spot elimination, as well as a more tightly regulated server temperature all lead to reduced cost of operation over the long haul, as well as improved server life and uptime.

1.2.3 Off-Peak Thermal Storage

An entirely different approach to cooling efficiency improvement is the use of ice as a thermal storage medium from which the requisite peak-load cooling can be drawn. By using the chiller cooling capacity to freeze water during off-peak times and storing the ice for later use, the chiller can be run less frequently during peak-load. During times of peak-load, the ice storage is used to chill the water that circulates through the CRAC units, which reduces the chiller compressor operation. The two-fold rationale behind ice storage lies in the fact that power companies charge a premium for power usage during hours of peak demand and ambient wet bulb temperatures are generally lowest during non-peak demand hours. Therefore, by utilizing the chiller during hours of lowest power demand, data centers can enjoy reduced energy usage because of increased chiller efficiency, and decreased cost of power. Also, the chiller can be intelligently undersized and only operated at optimal efficiency when needed for supplemental, peak data center load cooling [8]. However, a major limitation of this approach is the

dependence on locale. That is, the local cost of energy and annual ambient temperatures can greatly affect the profitability of utilizing a large scale thermal storage system.

1.2.4 Waste Heat Recovery

The alternate cooling methods mentioned so far focus on improving the efficiency of cooling systems by reducing undesirable air flow dynamics, or by reducing and storing cooling capability during off-peak energy demand hours to reduce the cost of electricity during peak demand. In contrast, a waste heat recovery system utilizes the heat generated by the servers. Many waste heat recovery techniques have been investigated in the past, but among the more common methods available are the organic rankine cycle, thermoelectric generation, and the ejector.

1.2.4.1 Organic Rankine Cycle (ORC)

The organic rankine cycle (ORC) utilizes an organic fluid with a boiling point lower than that of water in order to generate useful energy, such as electricity. Waste heat is used to vaporize the working fluid, causing the pressure and temperature of the fluid to increase. The fluid is then passed through a turbine, which generates electrical power via a shaft. The fluid depressurized vaporized fluid is then passed through a condenser, and is pumped back through the vaporizing chamber. Typical waste heat applications for the organic rankine cycle utilize heat at temperatures between 200°C and 500°C [9]. The organic rankine cycle is shown graphically in Figure 4.

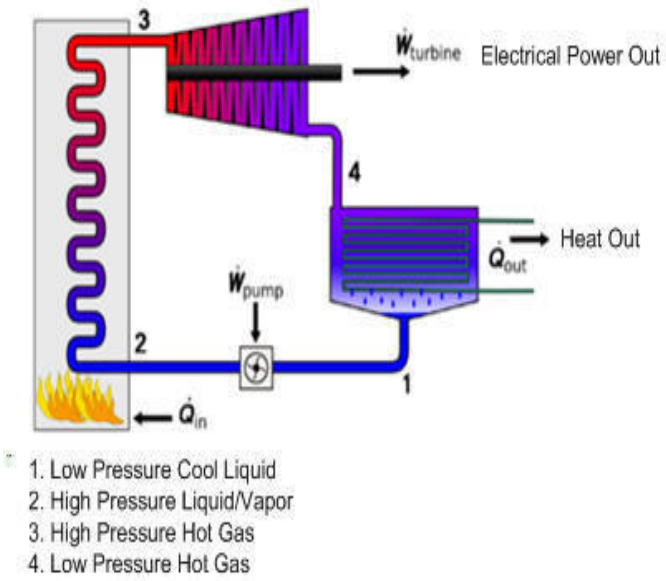

Figure 4. Organic Rankine Cycle Diagram (Courtesy of Tran Pacific Energy)

1.2.4.2 Thermoelectric Generation (TEG)

Operating based on the Seebeck, Peltier, and Thomson effects, thermoelectric devices can be configured to create a small electric current based on the temperature difference between its two surfaces. The generation efficiency of thermoelectric devices is typically relatively low. For computer server operating temperatures (70°C to 75°C), the power generation can be as low as 5 mW for 80 W of input power, or approximately 0.006% [10]. While thermoelectric devices might be suited for hot spot reduction, the low level of power generation reduces their applicability to the data center environment.

1.2.4.3 Ejector Based Refrigeration Cycle

Ejector based waste heat recovery is not a new subject. The absence of moving parts in ejectors has long attracted engineers who want a long lasting, continuous duty pumping device that can survive in hazardous environments, such as power plants [11]. With that in mind, large-scale ejector systems have been successfully developed for the recovery of waste heat from power plants, metal working facilities, and other sources [12]. The common parameter for these applications is consistently available high temperature waste heat, and/or a steady supply of heat

over time. Before going any further, let's look at the operational principles of the ejector, detailed graphically in Figure 5.

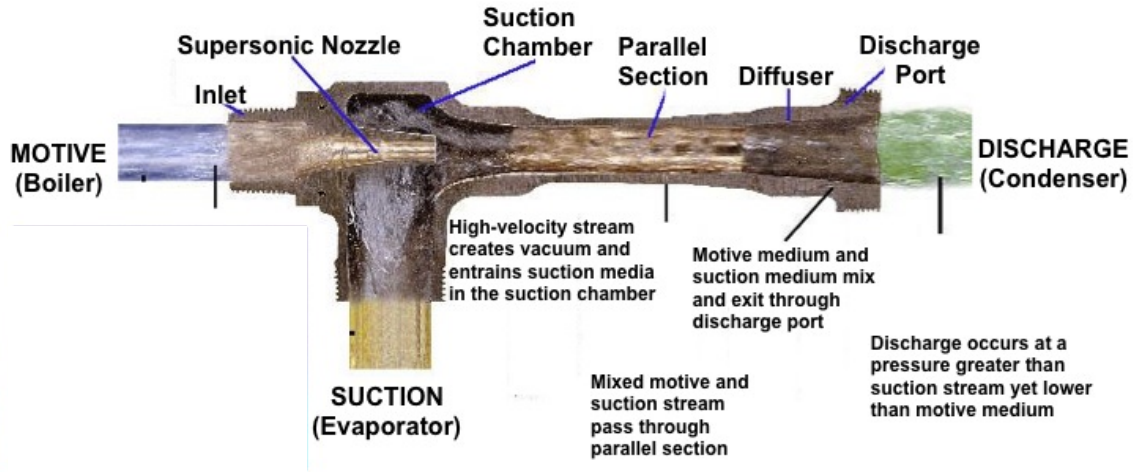

Figure 5. Cutaway of Ejector Illustrating the Principles of Ejector Operation (Courtesy of Penberthy)

The ejector is composed of two inlet ports (Motive and Suction) and one discharge port. The motive stream is a high temperature, high-pressure fluid, and the suction stream is a relatively low temperature, low-pressure fluid. The high pressure of the motive stream is converted into a supersonic jet, which entrains the low velocity suction fluid by the venturi effect [13]. The two streams mix in the mixing chamber, and then are discharged through the diffuser. The effect of the entrainment of the suction fluid and the diffusion of the mixed streams is a small compressive effect between the suction and the discharge ports. This compressive effect can then be used as a replacement of the conventional electro-mechanical compressor in a conventional vapor-compression refrigeration cycle. The refrigeration achieved can then be used for space cooling or for any other cooling application. A typical ejector based refrigeration cycle is shown in Figure 6.

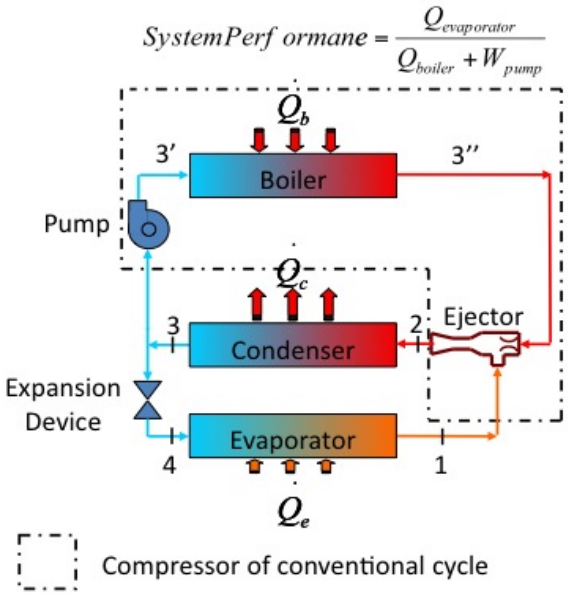

Figure 6. Conventional Ejector Refrigeration Cycle with System Performance

The cycle represented by 1-2-3-4 is the same as a conventional vapor-compression refrigeration cycle. The cycle represented by 2-3-3'-3'' is the power cycle of the ejector refrigeration cycle. A liquid pump raises the pressure of the motive fluid, and a high temperature heat source vaporizes the motive stream before it reaches the ejector. The ejector operates as described previously, and the compressed mixed stream passes through the condenser, splits, and continues the power cycle and the refrigeration cycle. By using a combined heat engine and refrigeration cycle model, shown below in 7, the system performance is found to be

$$System\ \ Performance = \frac{\overset{o}{Q}_{evp}}{\overset{o}{Q}_{boiler} + \overset{o}{W}_{pump}} \qquad 1$$

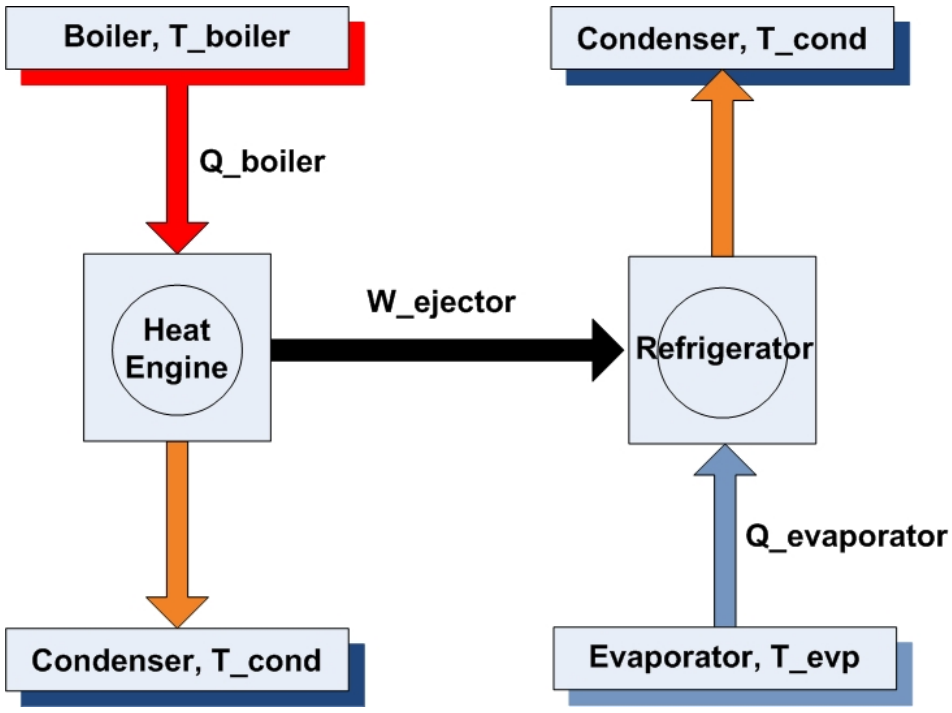

Figure 7. Thermodynamic System Depicted as Combined Heat Engine/Refrigeration Cycle

The Ejector Heat pump departs from a traditional vapor compression cycle at the compressor component. The traditional compressor is replaced with a pump, boiler and ejector components. The pump work is modeled using constant specific volume using Equation , as seen below.

$$W_{pump} = \dot{m} \cdot v \cdot (P_{out} - P_{in}) \quad 2$$

The boiler and evaporator are modeled as general heat exchangers. Performing an energy balance over the heat exchangers yields Equation , which is used to model the boiler as well as the evaporator.

$$Q_{input} = \dot{m} \cdot (h_{out} - h_{in}) \quad 3$$

After the pump raises the working fluid to the saturation pressure, the heat input, Q_{boiler}, changes the phase from liquid to vapor as it prepares to enter the Ejector component. Typical

performance values for ejector based refrigeration systems operating at typical data center conditions (heat source temperatures between 70 and 75°C) are between 0.2 and 0.3, which is equivalent to approximately 20 to 30% waste heat recovery [14].A brief comparison of the major players in waste heat recovery is shown in Table 1. Considering the potential waste heat recovery efficiency from the ejector based system, the ejector seems to provide the highest return while operating within the confines of the expected data center temperatures.

Table 1. Summary of Common Waste Heat Recovery Methods, Temperatures, and Efficiencies

Method	Heat Source Temperature	Efficiency
ORC	200-500°C	up to 10%
TEG	50-75°C	up to 1%
Ejector	65-85°	up to 30%

1.3 Ejector Literature Review

A detailed literature review was conducted to investigate the current experimental results for ejector based refrigeration systems. The review was split into ejector applications with waste heat temperatures greater than 100°C and ejector applications with waste heat temperatures less than 100°C, with a greater focus on those below 100°C. This literature review provides a summary of various works using various working fluids.

Boumaraf and Lallemand conducted experiments using refrigerants R-142b and R-600a as working fluids with boiler, evaporator, and condenser temperatures of 120-130°C, 10°C,and 20-35°C, respectively. The main focus of their work was on the effects on operating at off-design operating conditions, a scenario of prime interest to an ejector applied to the data center environment due to the dynamic nature of the temperatures in data centers. Their findings showed an ejector should be sized based on the highest anticipated hot source temperature in order to ensure operation over lower hot source temperatures as well. Even when operating at off-design conditions, the system was able to achieve a COP of 0.07-0.125 [15].

Chunnanond and Aphornratana very successfully achieved refrigeration using steam as the working fluid and was able to maintain a COP between 0.29 and 0.5 with boiler, evaporator, and condenser temperatures of 120-135°C, 10°C, and 20-35°C, respectively. The paper also details the importance of maintaining a condenser pressure below the critical pressure, which ensures optimal operation. The focus of their work was on the flow characteristics of the ejector, specifically the effects of condenser pressure and ejector primary nozzle throat diameter [16].

Khalil, A., et al., developed a model to predict the performance of an ejector system using R134a as the working fluid with boiler evaporator and condenser temperatures of 65-80°C, 0-10°C, and 25-40°C, respectively. The authors present conclusions about the geometrical effects, nozzle efficiency, as well as the effects of increasing the boiler temperature. The model showed that by increasing the boiler temperature by 5°C, the COP could be improved by 56%. Also, higher evaporator temperatures cause increased sensitivity of the entrainment ratio and COP to the boiler temperature [12].

Yapici, R., et al., performed experimental tests on an ejector system using R123 as the working fluid. The boiler, evaporator, and condenser temperatures were 83-103°C, 10°C, and 34°C, respectively. The specific purpose of the tests was to experimentally determine the optimum boiler temperature with respect to the ejector area ratio $\left(\frac{d_{mixing}}{d_{throat}}\right)^2$. Additionally, it was found that the COP of the system decreases dramatically when the boiler temperature is moved away from the optimum temperature. Finally, it was found that there is an optimum boiler temperature for every area ratio [17].

Meyer, A.J., et al., conducted small scale experiments on a steam jet ejector refrigeration cycle for the purpose of air conditioning. The boiler, evaporator, and condenser temperatures were set at 85-140°C, 5-10°C, and 15-35°C, respectively. The most important find from the

perspective of this thesis is the COP of 0.253 achieved with a boiler temperature of 95°C, a possible heat source temperature of future servers if current operating temperature trends continue [18]. If these temperature heat sources were available in the data center environment, a steam operated ejector system could provide low cost air conditioning to the computing servers with zero potential harmful effects to the environment or data center operators. Currently, however, steam systems still require a higher boiler temperature than is available in data centers.

The results of the ejector literature review are summarized in Table 2. In general, the steam based systems require higher temperature heat sources (>100°C), whereas the refrigerant based systems can operate with lower temperature heat sources (<100°C). Yapici, R., et al. achieved respectable performance using R123 and operating conditions similar to those observed in a data center. Since R123 is no longer legal in the United States based on the Environmental Protection Agency's ozone-depletion reduction policy, a suitable alternative was evaluated by constructing a model that could test the performance of working fluid candidates.

Table 2. Summary of Ejector Review by Temperatures

References	Boiler Temperature [°C]	Evaporator Temperature[°C]	Condenser Temperature [°C]	Working Fluid	COP
Boumaraf and Lallemand (2009)	120-130	10	20-35	R142b and R600a	0.07-0.125
Chunnanond and Aphornratana (2004)	110-150	5-15	100	Steam	0.29-0.5
Khalil, A., et al (2010)	65-85	0-10	25-40	R134a	0.05 -0.25
Yapici, Ersoy, Aktoprakoglu, Halkaci, and Yigit (2008)	83-103	10	34	R123	0.27-0.4
Meyer, Harms, and Dobson (2008)	85-140	5-10	15-35	Steam	0.2-0.26

2. EJECTOR MODEL AND SYSTEM DEVELOPMENT

As stated earlier, historical applications of the ejector based waste heat recovery systems have been mostly successful in environments that have a large amount of high temperature waste heat available. Data centers, on the other hand, due to the temperature constraints of server components and human access requirements, only provide relatively low temperature waste heat on the order of 50 to 80°C [19]. This creates a significant complication in ejector system design. While most ejector systems employ vaporized water as the working fluid, the temperatures found in data centers dictate the use of a secondary working fluid, preferably one with a low boiling point to achieve the optimal operating pressures for the ejector selected. Also, power plants and production facilities tend to have a more constant heat output over time, whereas a data center's heat generation varies throughout the day as servers are tasked and released.

2.1 Development of a Simplified Ejector Refrigeration System Model

In order to properly design an operable ejector based, waste heat driven refrigeration cycle, a simplified thermodynamic model was constructed using Engineering Equation Solver. The schematic representation of the system is shown graphically in Figure 8.

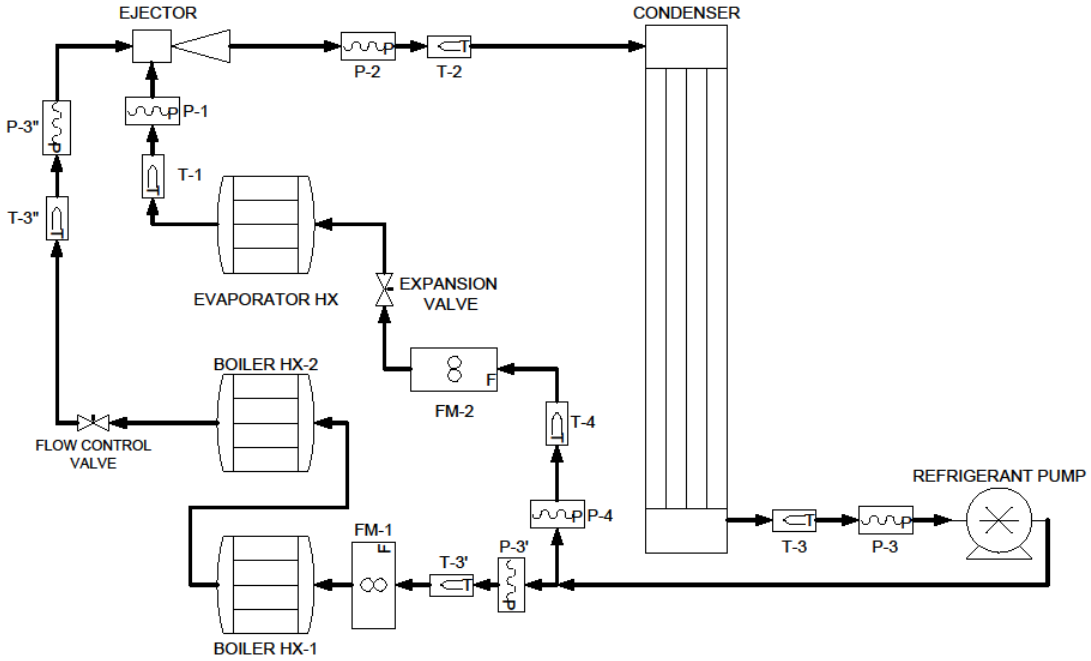

Figure 8. Ejector System Schematic with Key Components Marked

Table 3. Key System Component Legend

FM-#	Positive displacement flow meter
P-#	Pressure transducer
T-#	Type T thermocouple
HX-#	Heat Exchanger

Internal EES functions were used to determine operating pressures based on user prescribed operating temperatures and saturation conditions. Recalling that the necessary parameters to determine the system performance are the heat input to the boiler and the evaporator and the work of the liquid refrigerant pump, the heat loads and pump work were determined by the following equations, respectively:

$$\dot{Q}_{VG} = \dot{m}_{VG} \cdot \left(h_{out} - h_{in}\right) \quad 4$$

$$\dot{Q}_{EVP} = \dot{m}_{EVP} \cdot \left(h_{out} - h_{in}\right) \quad 5$$

$$\dot{W}_{pump} = \dot{m}_{evp+VG} \cdot v \cdot \left(P_{out} - P_{in}\right) \quad 6$$

Next, the ejector problem and the flow rates were solved simultaneously by using the principle of conservation of total energy for control volumes, shown in Equation 5 which in this case eventually simplifies to momentum balance [20].

$$\frac{dE}{dt} = \dot{Q} - \dot{W} + \sum \dot{m}_{in} \cdot \left(h_{in} + \frac{V_{in}^{\ 2}}{2} + gz_{in}\right) - \sum \dot{m}_{out} \cdot \left(h_{out} + \frac{V_{out}^{\ 2}}{2} + gz_{out}\right) \qquad 7$$

By assuming no heat transfer and no outside work done on the control volume, as well as negligible potential energy change and steady state, the energy conservation equation reduces to Equation 6.

$$\sum \dot{m}_{in} \cdot \left(h_{in} + \frac{V_{in}^{\ 2}}{2}\right) = \sum \dot{m}_{out} \cdot \left(h_{out} + \frac{V_{out}^{\ 2}}{2}\right) \qquad 8$$

Assuming that the flow velocity at the inlet of the motive port of the ejector is negligible, the energy balance over the motive nozzle control volume reduces to Equation 7, which includes the ejector motive nozzle efficiency. The energy of the flow stream can then be related to the momentum through the velocity of the stream by performing an energy balance over the entire internal ejector control volume, resulting in Equation 9.

$$\frac{V_{motive}^{\ 2}}{2} = k_{e,motive} = \eta_{nz} \cdot \left(h_{nz,in} - h_{nz,s}\right) \qquad 9$$

$$V_{motive} = \sqrt{2 \cdot k_e} \qquad 10$$

$$V_{comb} = \frac{\dot{m}_{VG}}{\dot{m}_{comb}} \cdot Vel_{motive} \qquad 11$$

In the above equations, k_e is the kinetic energy of the stream after the motive nozzle, η_{nz} is the motive nozzle efficiency, and V_{motive} is the velocity of the motive stream after the nozzle, and V_{comb} is the velocity of the mixed motive and suction streams before the diffuser at the discharge

port of the ejector. From here, the velocity of the mixed stream can be related to the kinetic energy of the mixed stream by

$$k_{e,comb} = \frac{V^2_{comb}}{2} \tag{12}$$

which can then be related to the enthalpy of the mixed stream by the energy equation. That is,

$$\dot{E}_{comb} = \dot{E}_{VG} + \dot{E}_{evp} \tag{13}$$

which can be rewritten as

$$\dot{m}_{comb} \cdot \left(h_{comb} + k_{e,comb}\right) = \dot{m}_{VG} \cdot \left(h_{VG} + k_{motive}\right) + \dot{m}_{evp} \cdot \left(h_{evp}\right) \tag{14}$$

Solving for the enthalpy of the combined flow yields

$$h_{comb} = \frac{\dot{m}_{VG} \cdot \left(h_{VG} + k_{e,motive}\right) + \dot{m}_{evp} \cdot \left(h_{evp}\right)}{\dot{m}_{comb}} - k_{e,comb} \tag{15}$$

which can then be used to complete the solution of the ejector problem by applying standard diffuser equations to determine the discharge pressure of the ejector. Since the rest of the system is essentially nothing more than a vapor-compression cycle, the system states can now be solved by the model.

2.2 Model Results: Working Fluid Selection

With the model completed, the next major step in the design process was to determine the appropriate working fluid. Recall that an important feature of the working fluid are a low boiling point for use with low temperature applications, good heat transfer characteristics, and environmentally benign. After sifting through various refrigerants and other fluids using the fluid database imbedded in EES, the following were selected for in-depth evaluation: R-134a, FC-72, and R-245fa. The resulting thermodynamic states for each refrigerant are listed below in Figures 9-11.

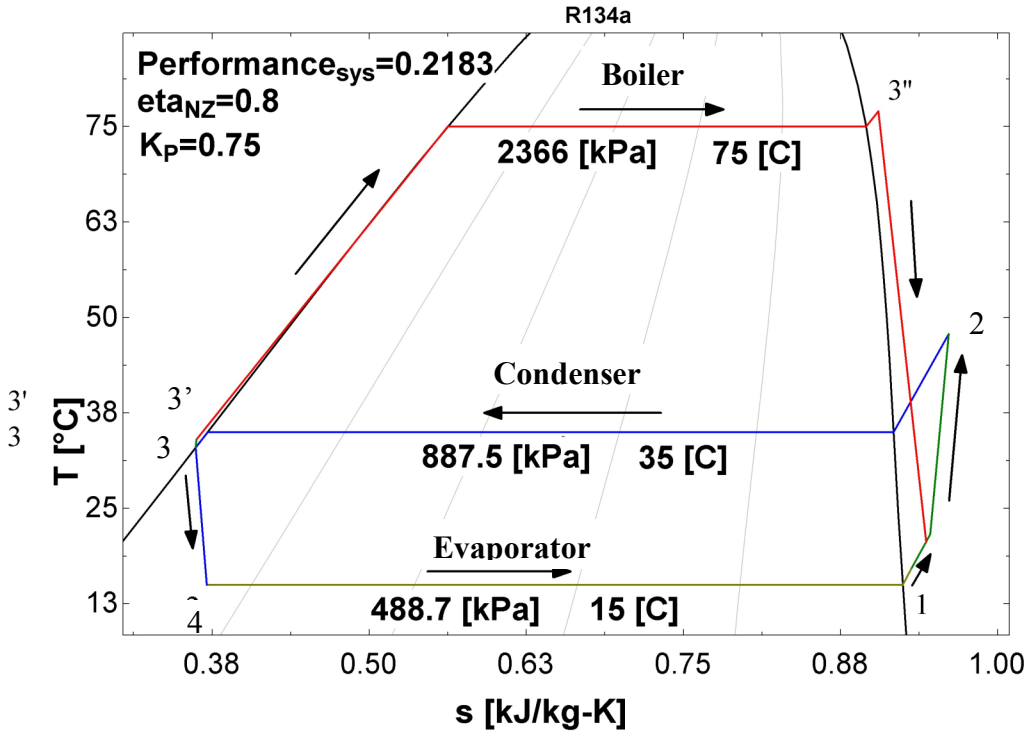

Figure 9. T-s Chart using R-134a as Working Fluid, Ideal Performance

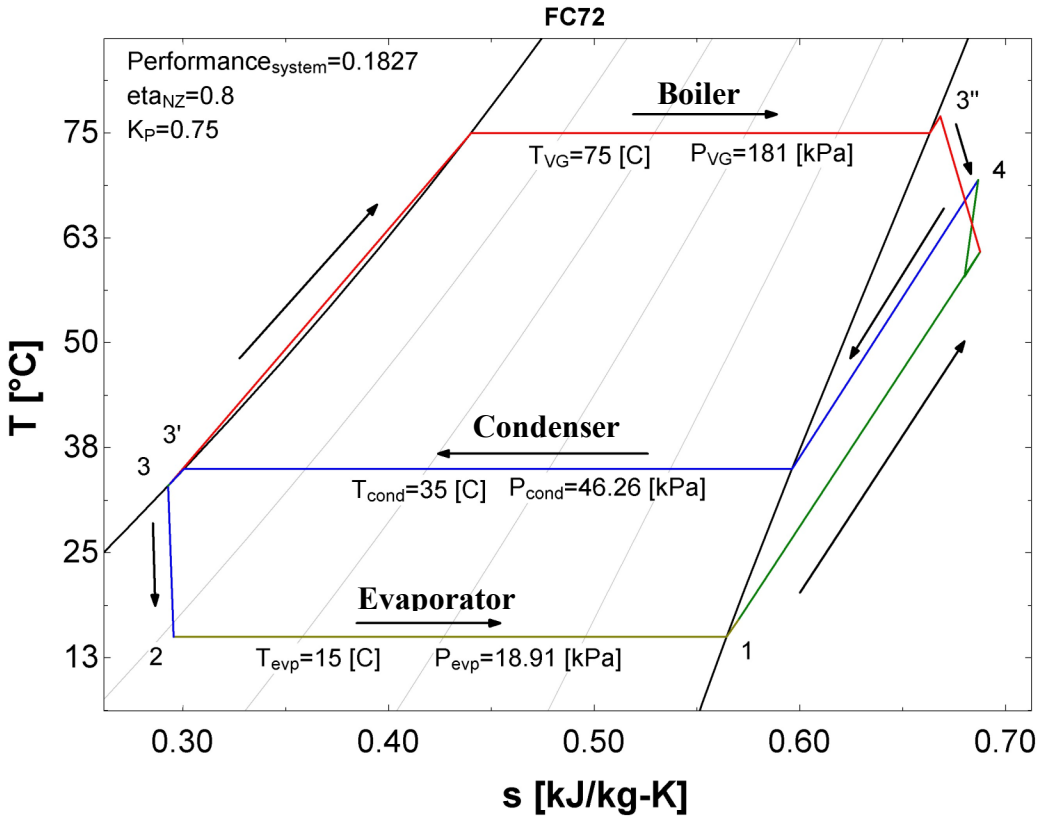

Figure 10. T-s Chart using FC-72 as Working Fluid, Ideal Performance

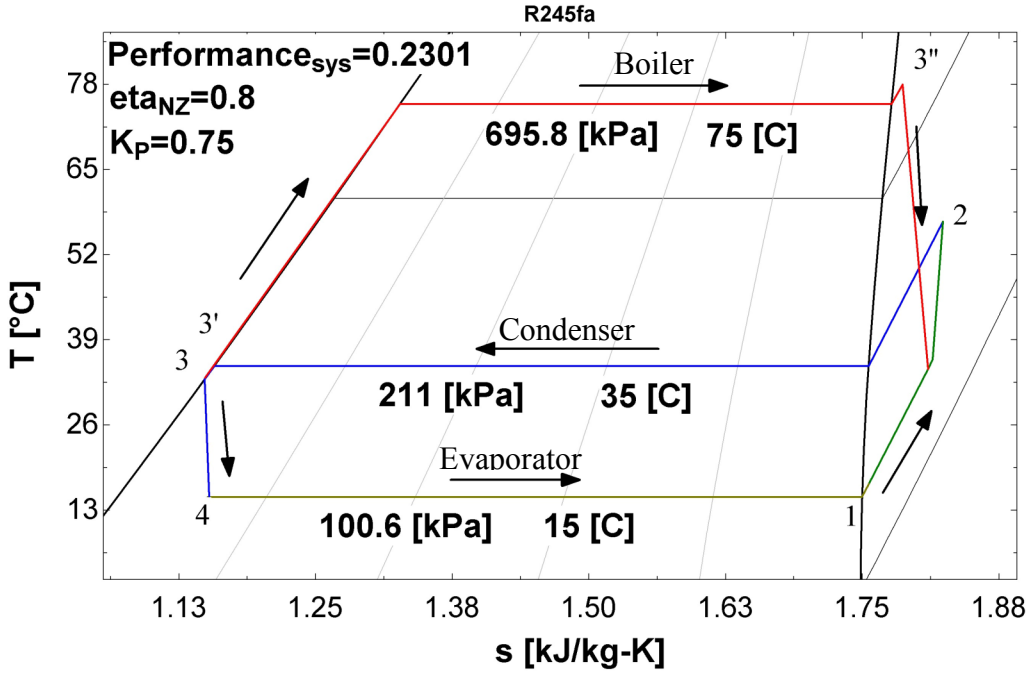

Figure 11. T-s Chart using R-245fa as Working Fluid, Ideal Performance

Referring to Figures 9-11, it is apparent that R-245fa has the highest performance due to the low temperature boiling point and the beneficial shape of the vapor dome. Taking into account working fluid selection factors, such as heat transfer properties, and health risks, R-245fa was selected as the working fluid and was examined in greater detail. A summary of pertinent properties is shown in Table 4.

Table 4. Summary of Working Fluid Candidate Properties at 101 kPa

Fluid	Boiling Point [°C]	Thermal Conductivity, Liquid [W/m-K]	Viscosity [mPa-s]	h_fg [kJ/kg]
R-134a	-25.9	0.0824	0.202	217.2
fc-72	56	0.057	0.64	88
R-245fa	15.3	0.085	0.431	200

2.3 Model Results: R-245fa-Ejector Performance Analysis

With the thermodynamic system defined and the working fluid selected, attention was directed toward ejector sizing and configuration. The two sizing approaches considered were ejector priority sizing and system priority sizing.

When using the ejector priority sizing method, the ejector is sized based on a desired performance with user selected fluid parameters at the motive and suction ports of the ejector (refer to Figure 5). The condenser, boiler, evaporator and other components are then sized based on the selected ejector. The advantage of this method is the ejector can be optimized based on specific operating parameters. The downside, however, is the potential lack of ejector manufacturers willing to fabricate custom ejectors, and the resources required to design, build, and verify the performance of a one-of-a-kind ejector.

When using the system priority sizing method, the system components are selected, and an ejector is selected that operates within the controllable parameter ranges of the other system components. This method allows for the use of an off-the-shelf ejector, which has performance data available from the manufacture, published sizing charts, and experienced support personnel.

Unfortunately, as mentioned before, most ejectors are designed for steam at extremely high temperatures and pressures, which results in non-ideal ejector performance at vastly different operating conditions. Even so, the system priority method was utilized in order to partially verify the reliability of the simplified ejector refrigeration system model as well as to have access to performance data that could be used if necessary.

After consulting Penberthy Ejectors' data sheets and engineering tools, ejector model GH-1 1/2 was found to have the greatest performance when operating at the a boiler temperature of 75°C, evaporator temperature of 15°C, and a condenser temperature of 35°C with an evaporator flow rate of 0.018 kg/s [21]. However, in order to provide the necessary motive and suction port flow rates, the total heat load of the system was increased to a design point of 40 kW in the boiler and 3 kW in the evaporator. Based on calculations using Equations 2 and 3, the flow rates for the boiler was predicted to be 0.18 kg/s. The system pressures were set at 700 kPa (abs), 210 kPa (abs), and 100 kPa (abs) for the boiler, condenser, and evaporator, respectively. With these conditions, the ejector was stated to provide a performance of approximately 0.07, or heat recovery of 7%. The modified model, plotted to reflect the expected performance from the manufacturer, is shown in Figure 12.

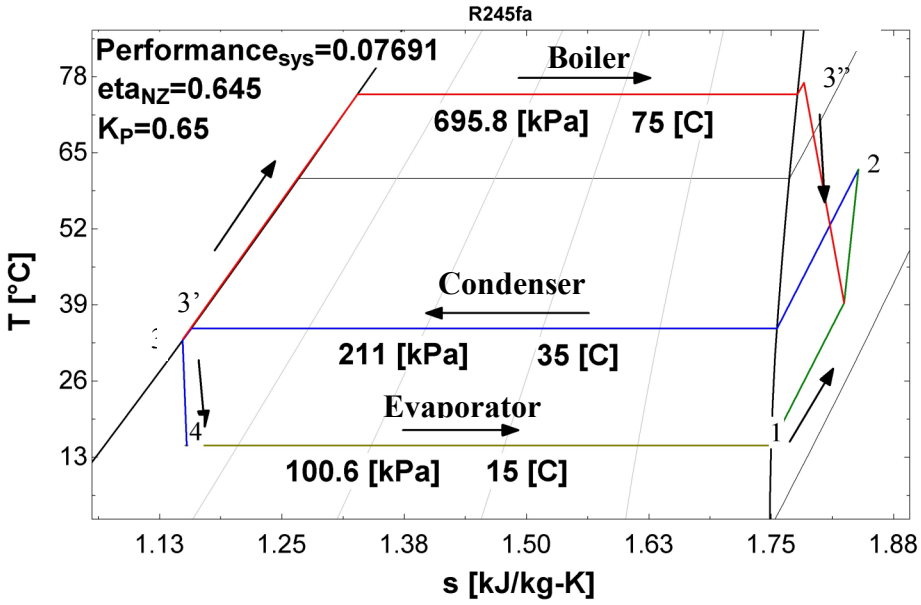

Figure 12. T-s Chart using R-245fa (Operating at Non-Ideal Performance)

While a return of 7% seems meager, it should be remembered that this energy would otherwise demand additional energy to cool, the ejector system process requires very little energy input, and this performance is achieved using a non-ideal ejector. For comparison, Figure 11 reflects the anticipated performance of an ideally designed ejector.

3. EXPERIMENTAL SETUP/RESULTS

The pressure and temperature sensors were carefully calibrated before the system was constructed. Utilizing precision, research grade calibrators, the thermocouples and pressure transducers were corrected in order to achieve pressure measurements with less than 0.2°C temperature error, and less than 0.5% error of the measured pressure value. National Instruments LabView Field Point modules were used to record the temperature and pressure data during calibration. The calibration setups for the temperature and pressure devices are shown graphically in Figures 13 and 14, respectively. The calibration curves for the thermocouples are shown in Figures 15-20 and the calibration curves for the pressure transducers are shown in Figures 21-26.

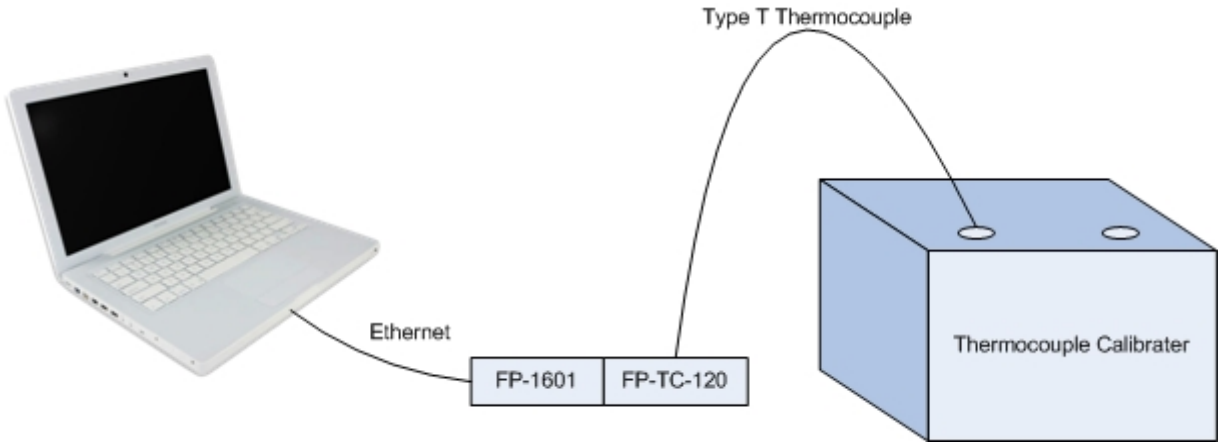

Figure 13. Thermocouple Calibration Setup with National Instruments FieldPoint Modules Used for Data Collection

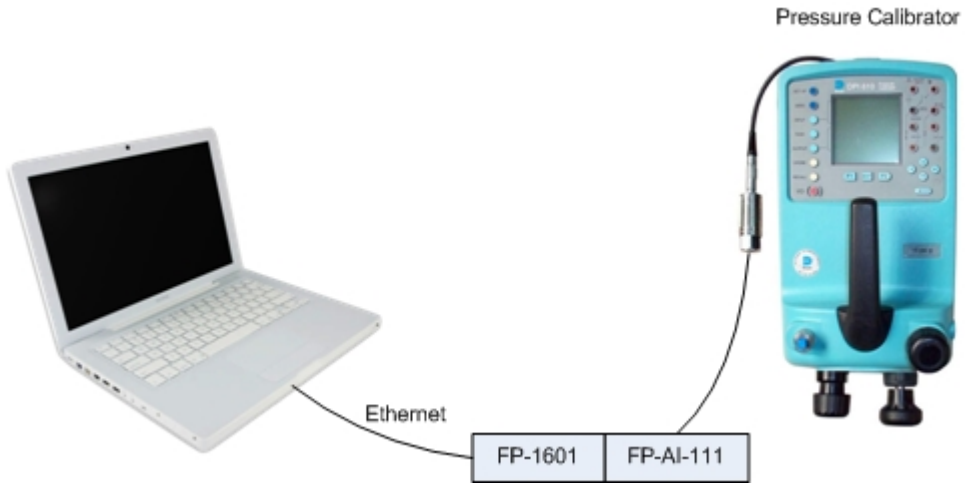

Figure 14. Pressure Transducer Calibration Setup with National Instruments FieldPoint Modules Used for Data Collection

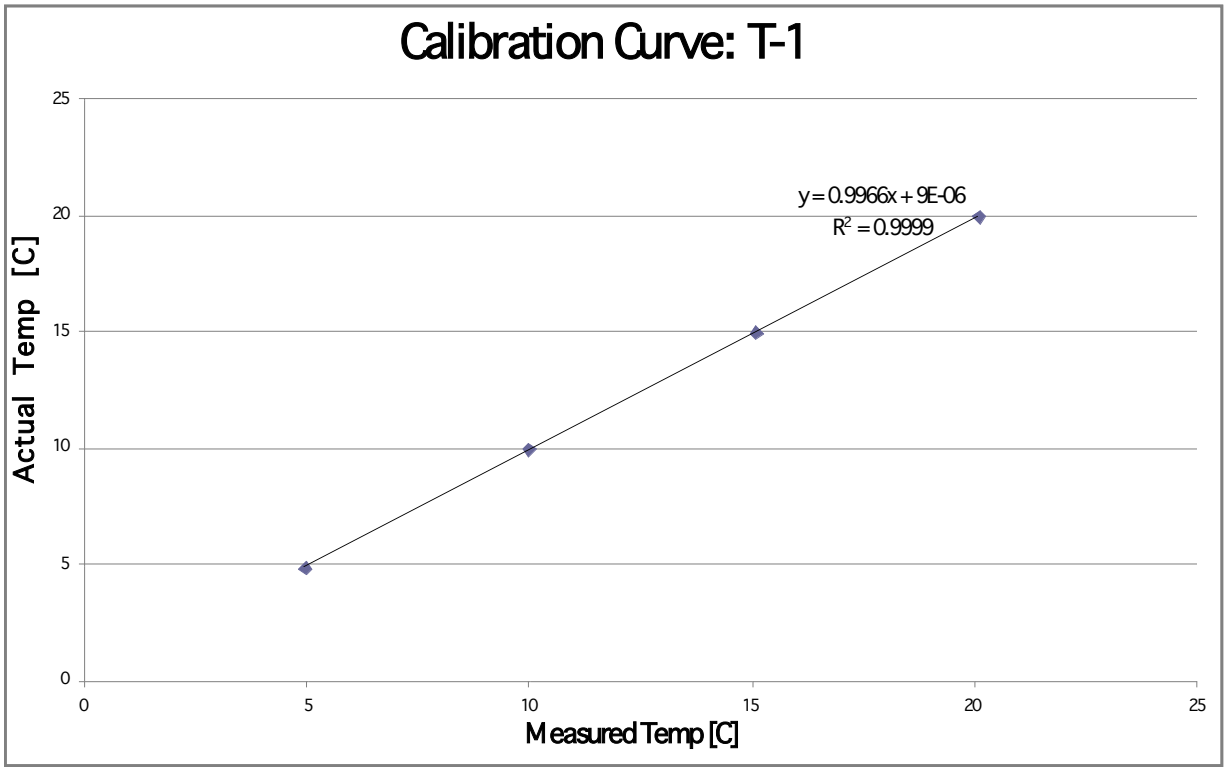

Figure 15. Temperature Calibration Curve for T-1 (Located in System at Evaporator Outlet)

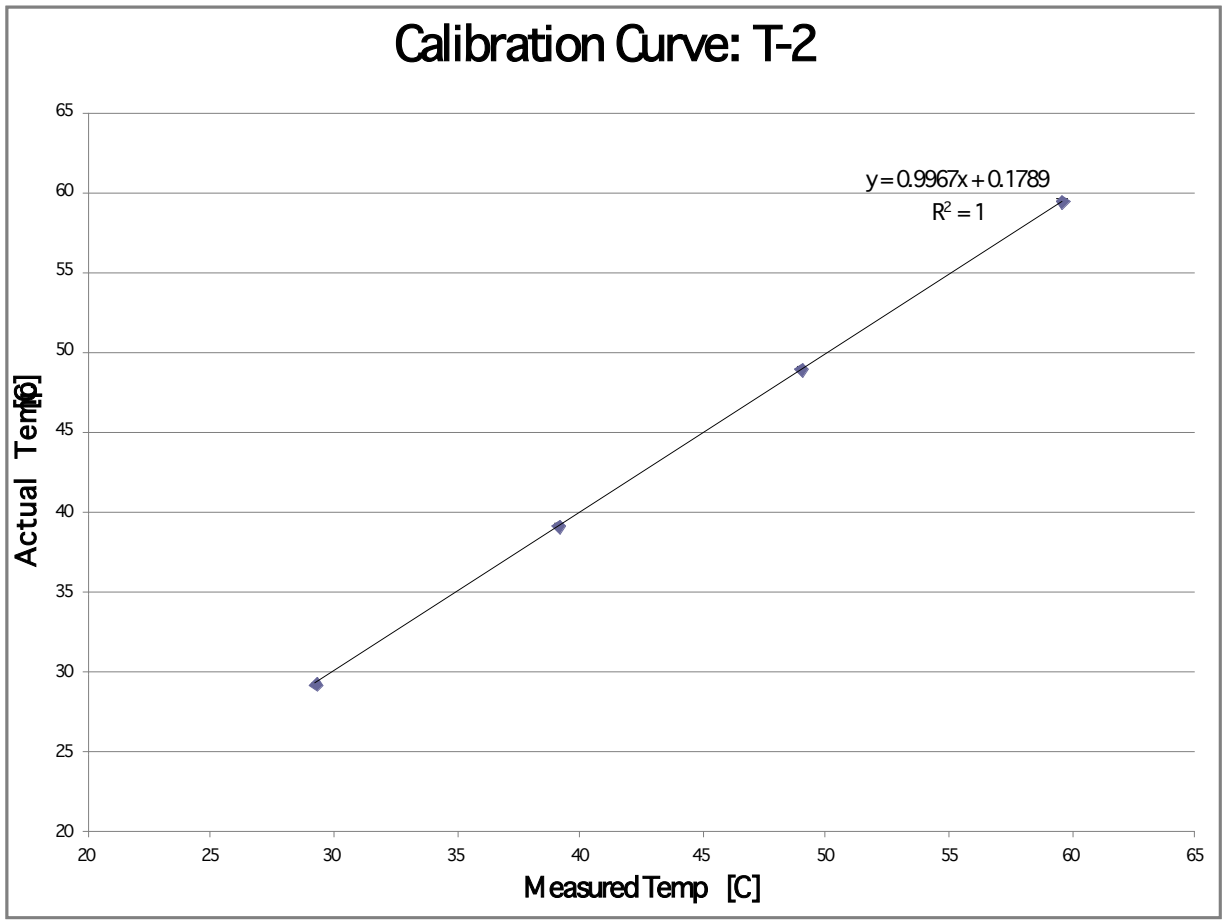

Figure 16. Temperature Calibration Curve for T-2 (Located in System at Condenser Inlet)

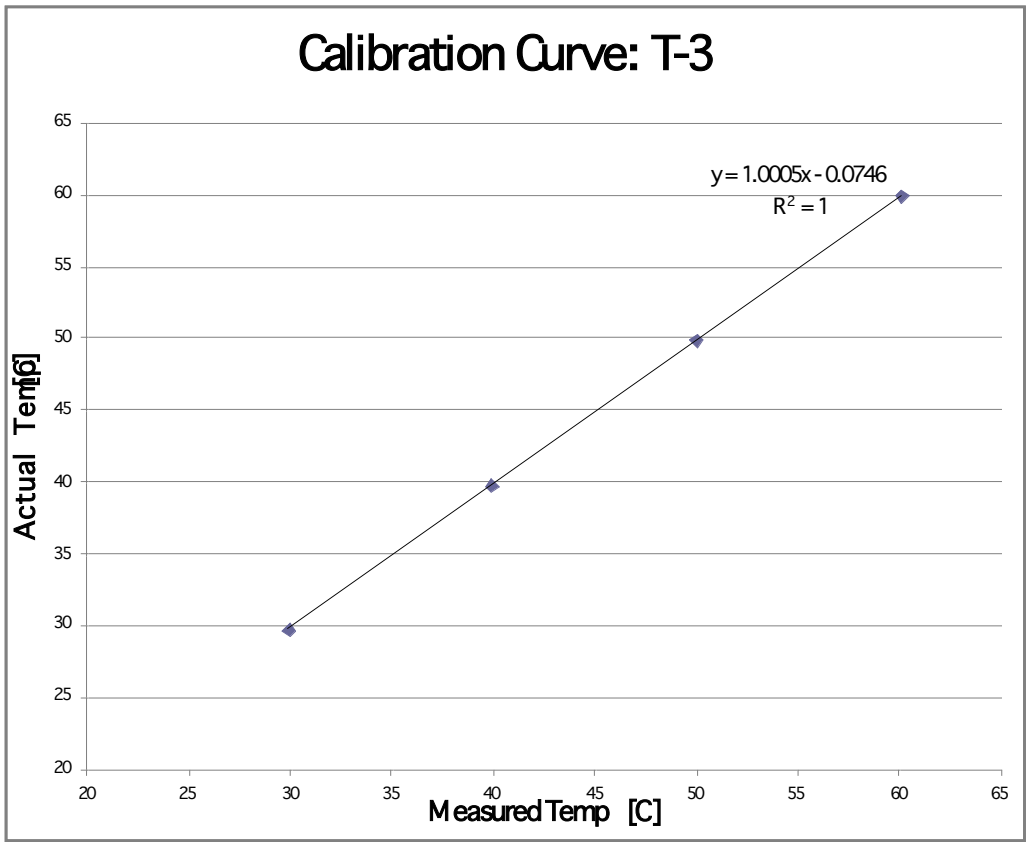

Figure 17. Temperature Calibration Curve for T-3 (Located in System at Condenser Outlet)

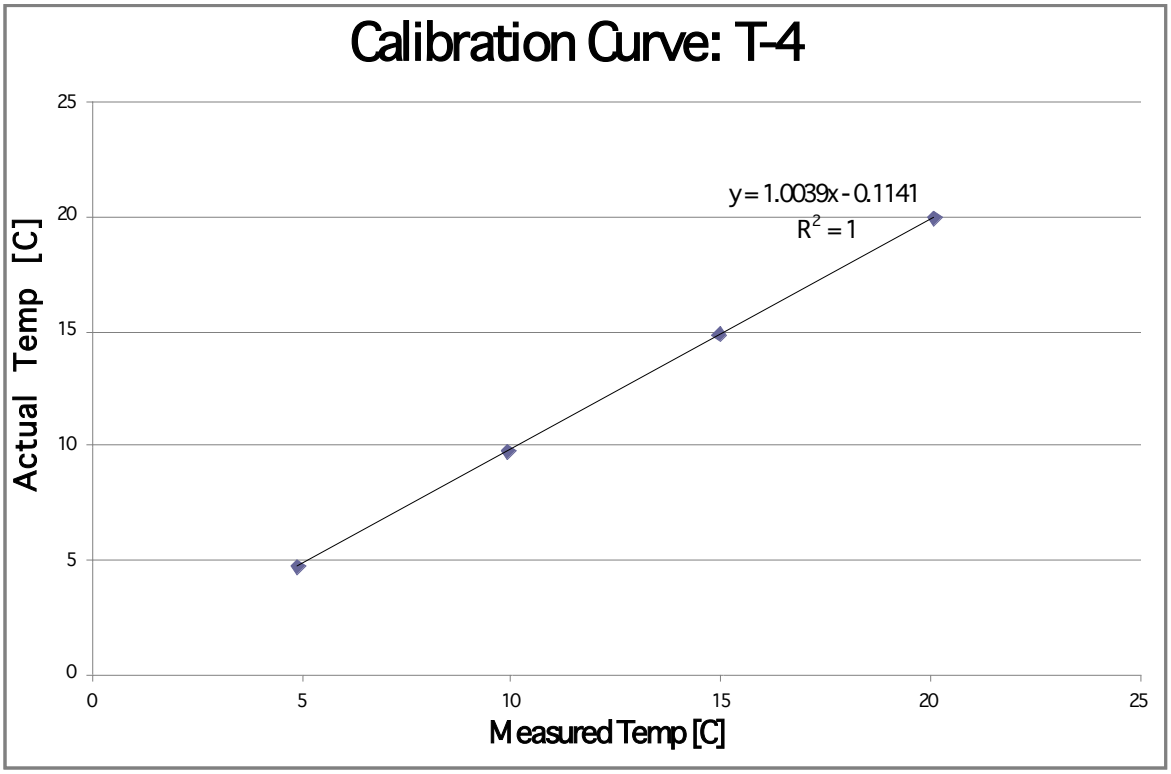

Figure 18. Temperature Calibration Curve for T-4 (Located in System at Evaporator Inlet)

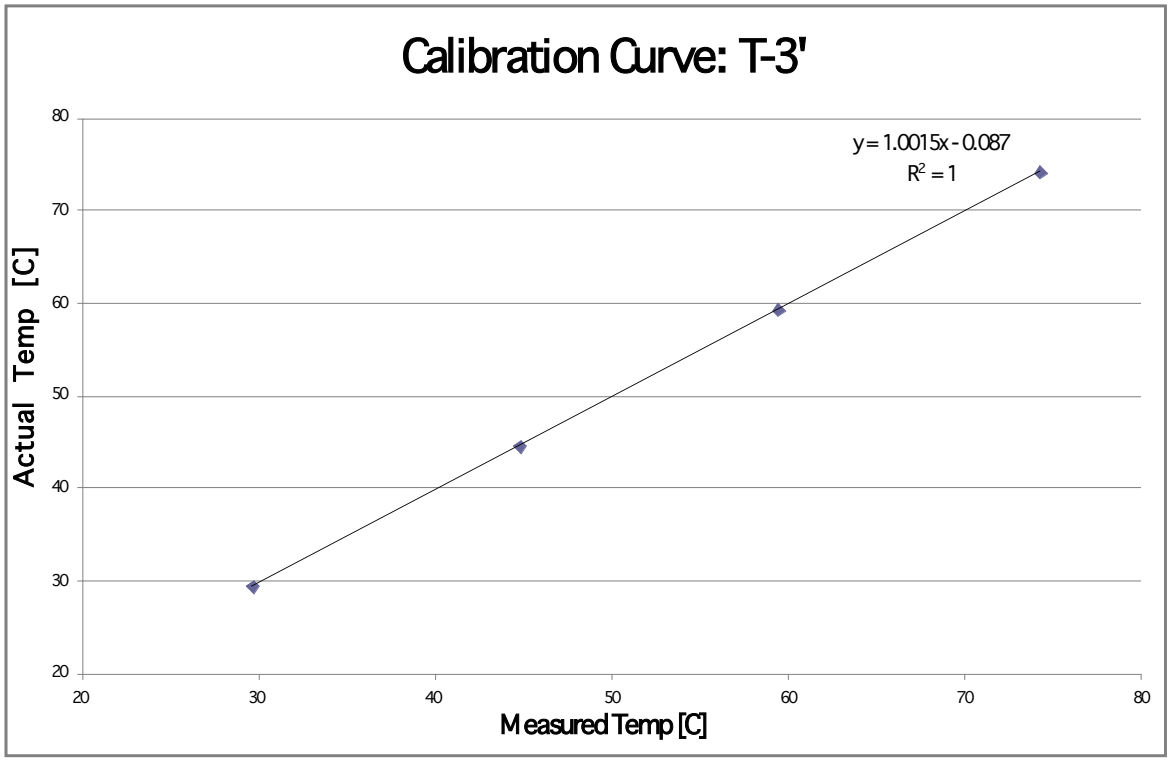

Figure 19. Temperature Calibration Curve for T 3' (Located in System at Boiler Inlet)

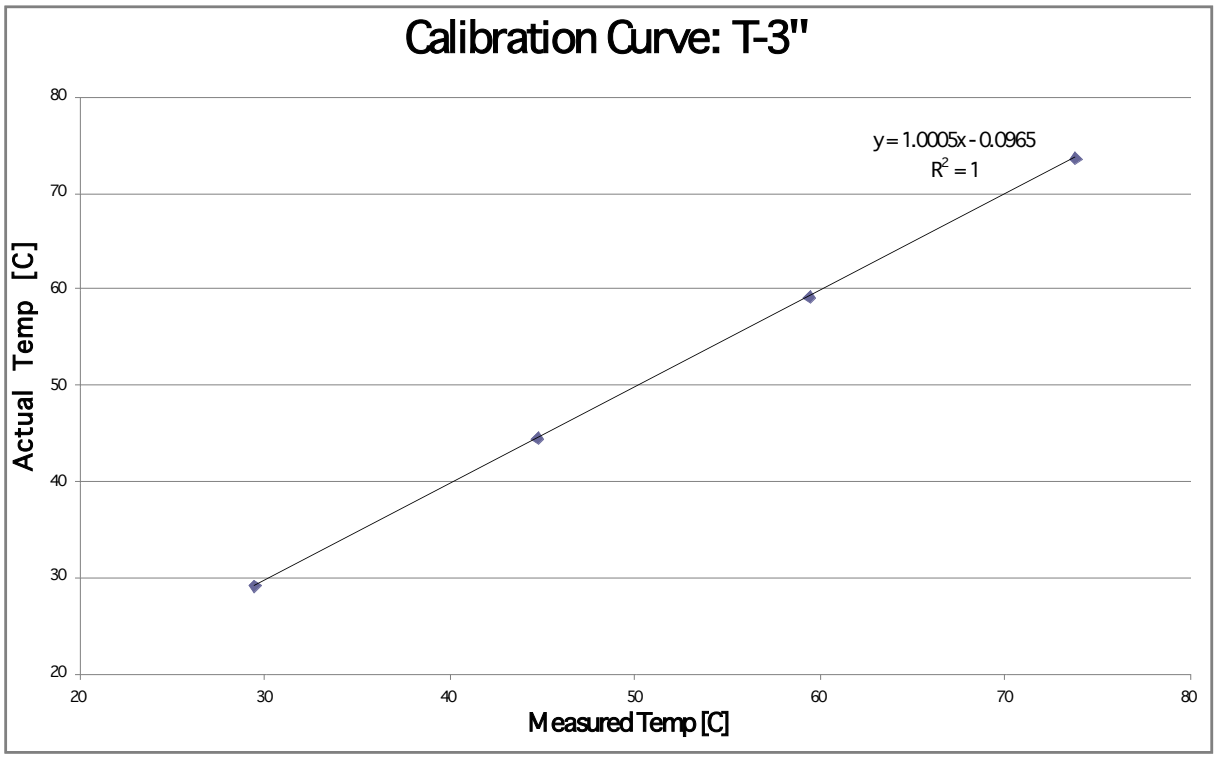

Figure 20. Temperature Calibration Curve for T-3" (Located in System at Boiler Outlet)

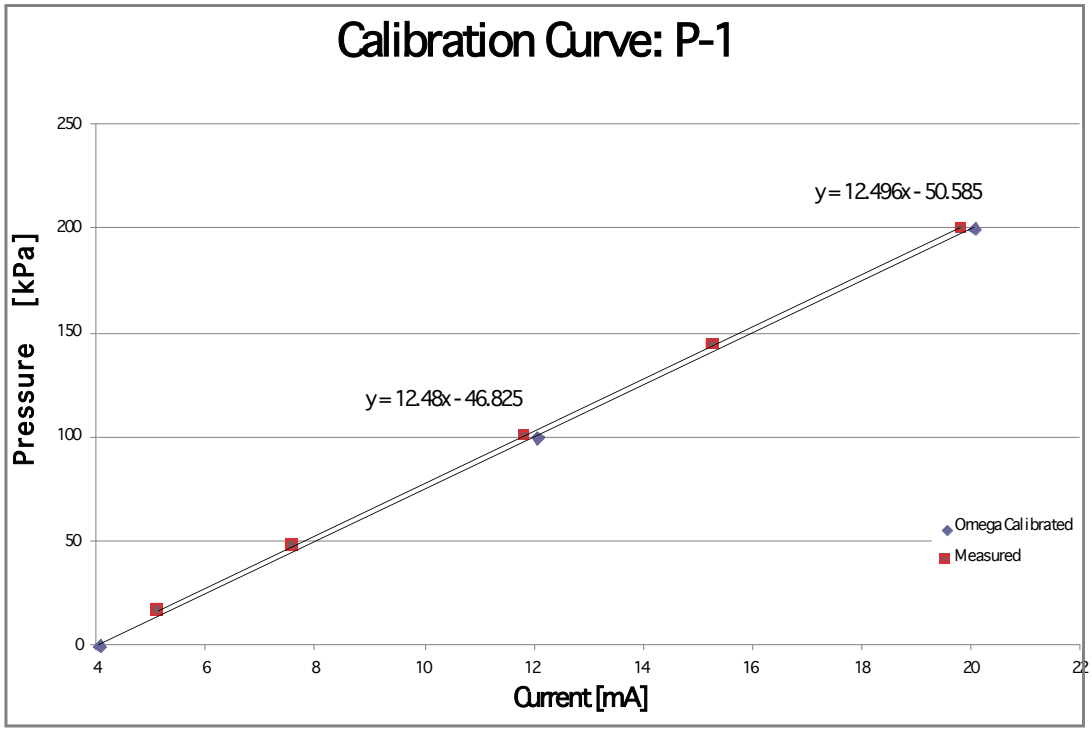

Figure 21. Pressure Calibration Curve for P-1 (Located in System at Evaporator Outlet)

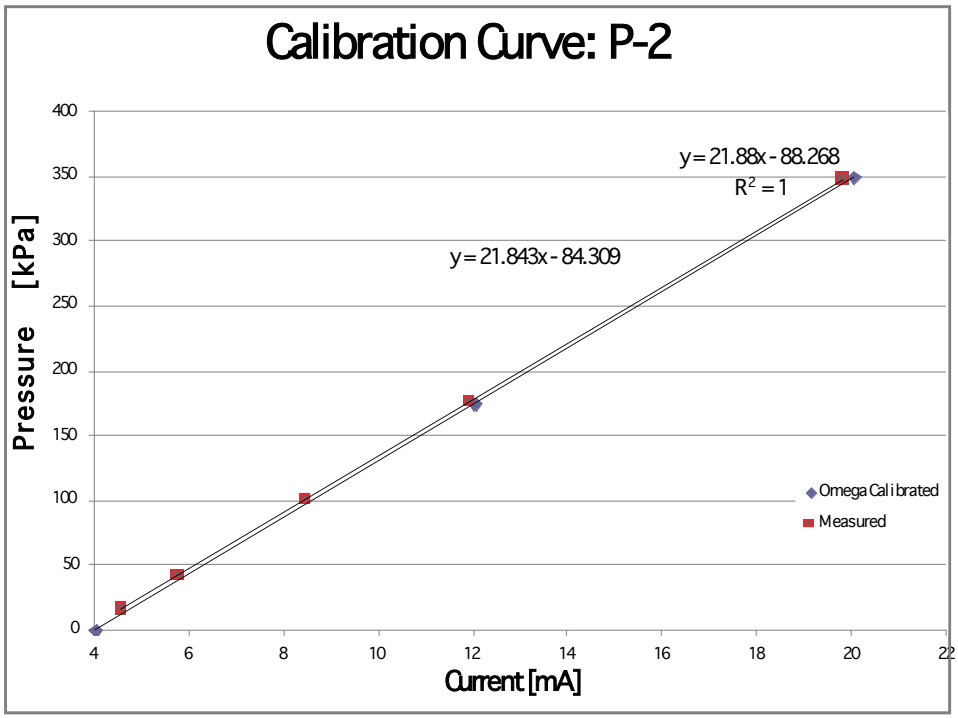

Figure 22. Pressure Calibration Curve for P-2 (Located in System at Condenser Inlet)

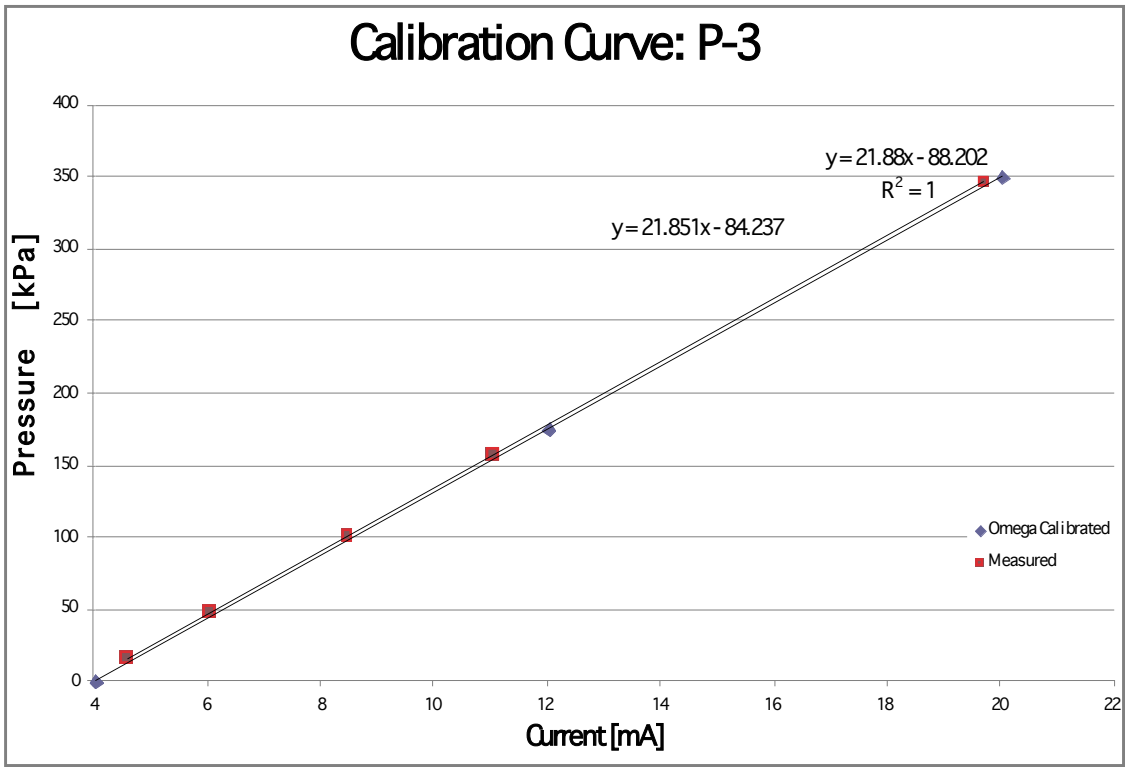

Figure 23. Pressure Calibration Curve for P-3 (Located in System at Condenser Outlet)

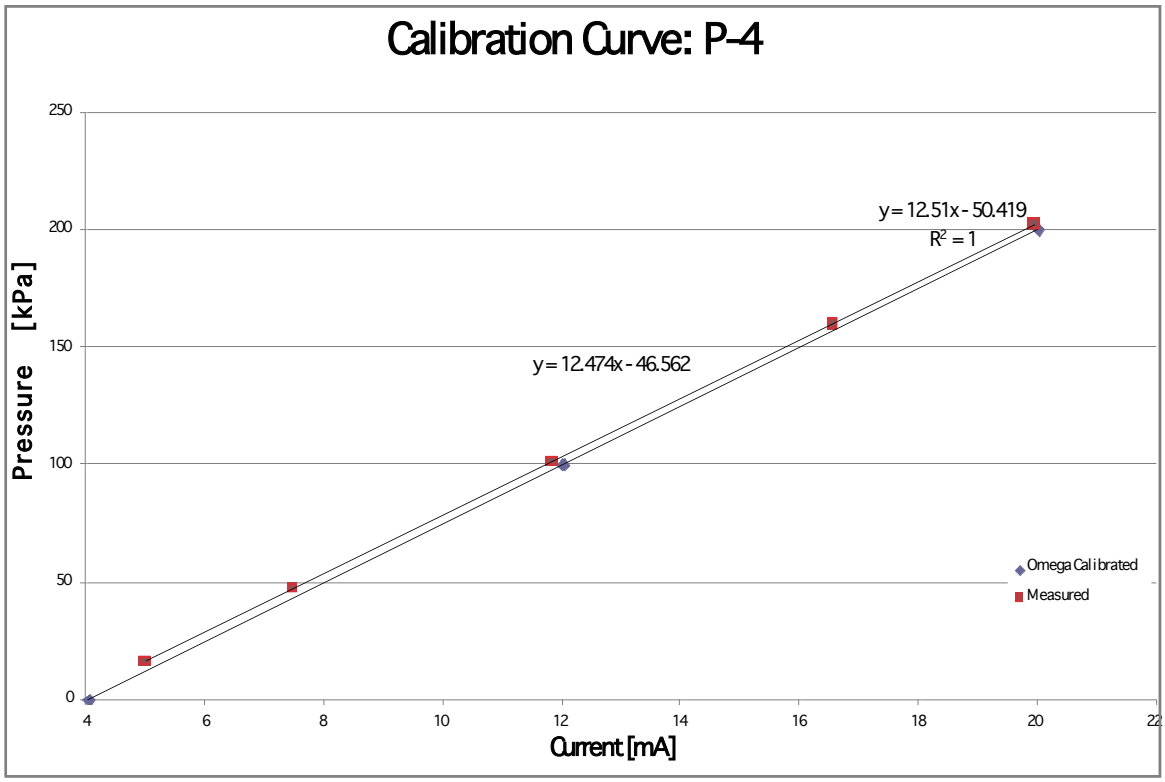

Figure 24. Pressure Calibration Curve for P-4 (Located in System at Evaporator Inlet)

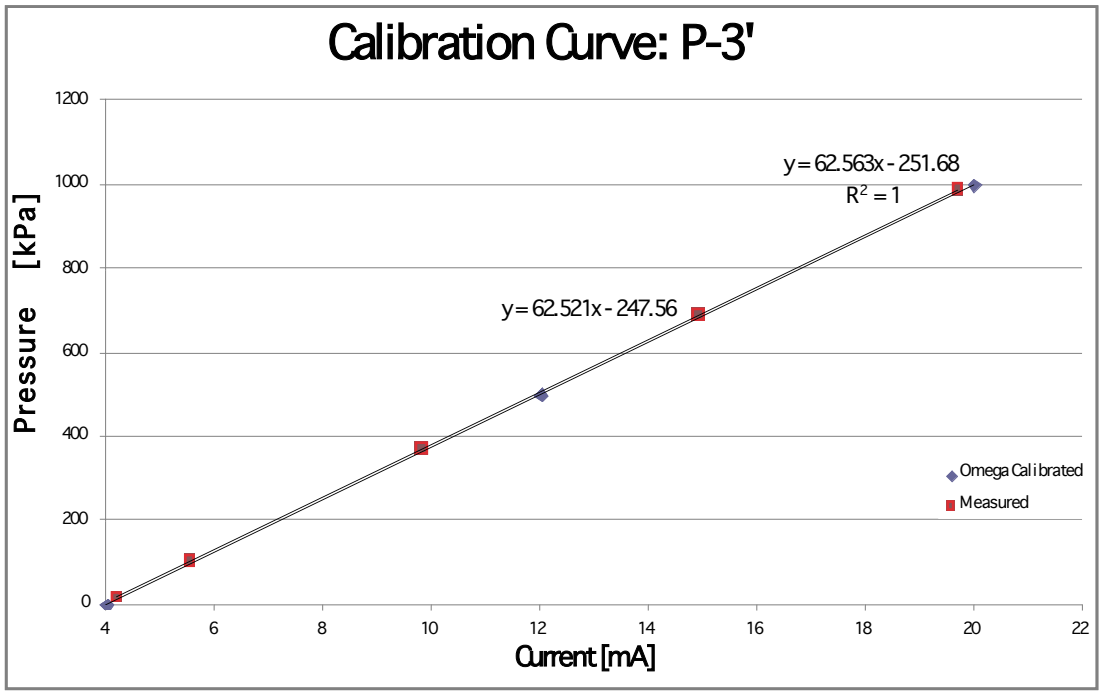

Figure 25. Pressure Calibration Curve for P-3' (Located in System at Boiler Inlet)

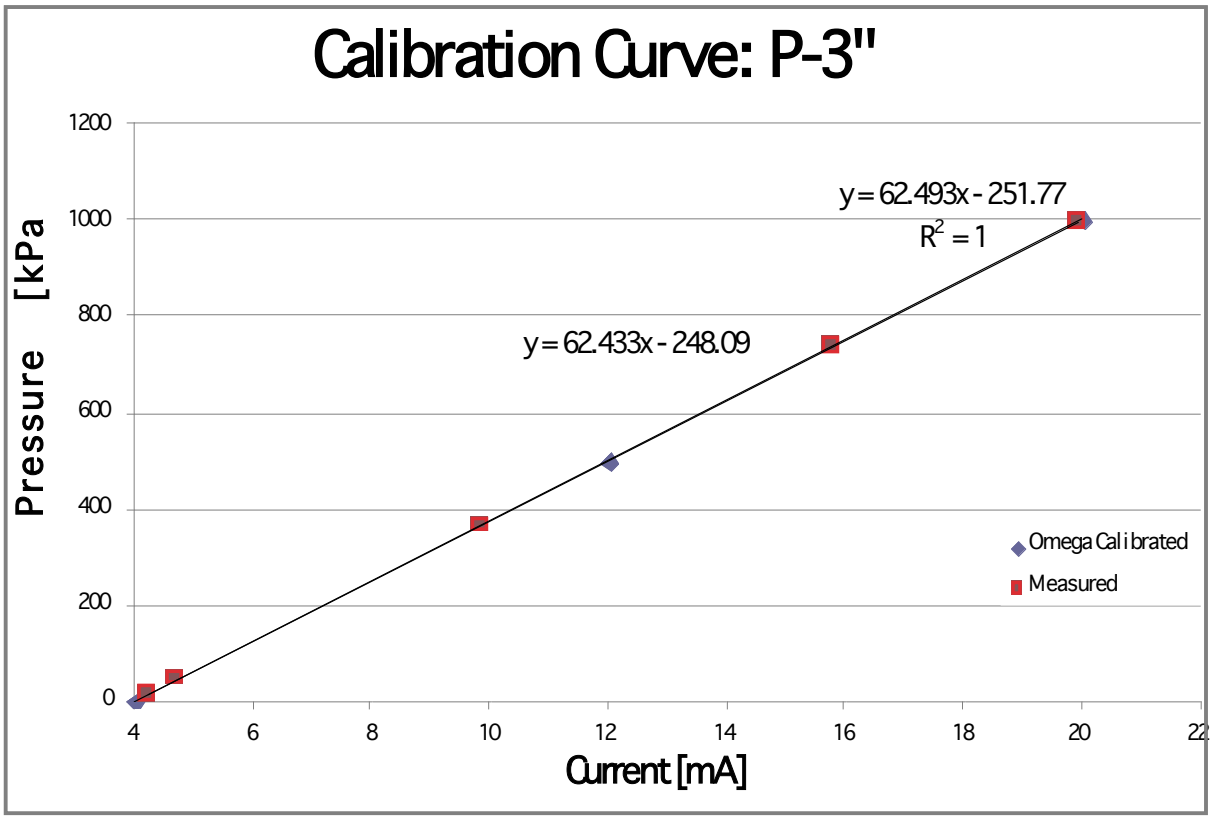

Figure 26. Pressure Calibration Curve for P-3" (Located in System at Boiler Outlet)

After calibrating the measurement instruments, the experimental system was constructed based on a schematic diagram, shown in Figure 27 and a more refined 3-D model, shown in Figure 28, to ensure rapid and accurate component placement and piping connections. Aluminum strut profiles were used for the mobile system platform, copper piping was used for most of the fluid connections, and Swagelok tube fittings ensured leak tight connections on both the refrigerant side and the hot water distribution side.

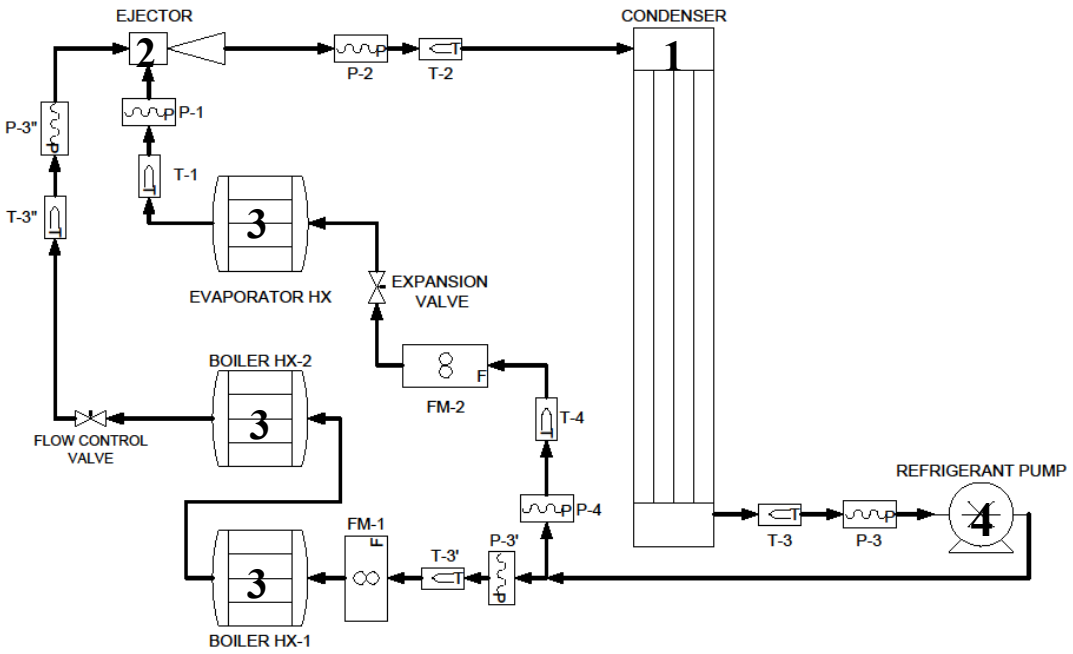

Figure 27. System Schematic with Key Components Marked

Table 5. Key System Component Designators

Component	Designator
Condenser HX	1
Ejector	2
Evaporator and Boiler HX	3
Refrig. Pump	4
Flow Meter	FM-#
Pressure Transducer	P-#
Thermocouple	T-#

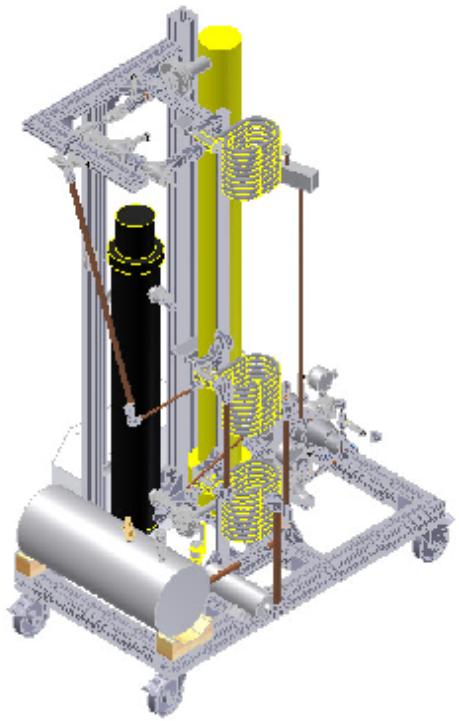

Figure 28. 3-D Model Representation of System Configuration shown in Figure 27 with Mobile Platform and Support Structure

3.1 System Details

As mentioned previously, the waste heat was simulated by using two water heaters: a hot water circulation heater for the motive stream heat input (boiler), and a water temperature control unit for the suction stream heat input (evaporator). The heaters were used to simulate the heat in order to provide control over waste heat which is harder to obtain from functioning servers. The heat input at the boiler was provided using a Durex, immersion style heater with a rated capacity of 40 kW, and the heat input at the evaporator was simulated using a Sterling temperature control unit with a rated capacity of 3 kW. On the heat rejection side of the system, a 43 kW capacity condenser was selected from Yula Corp and it served as the simulated heat rejection medium for the system. The various other components are visible below in Figures 29-33.

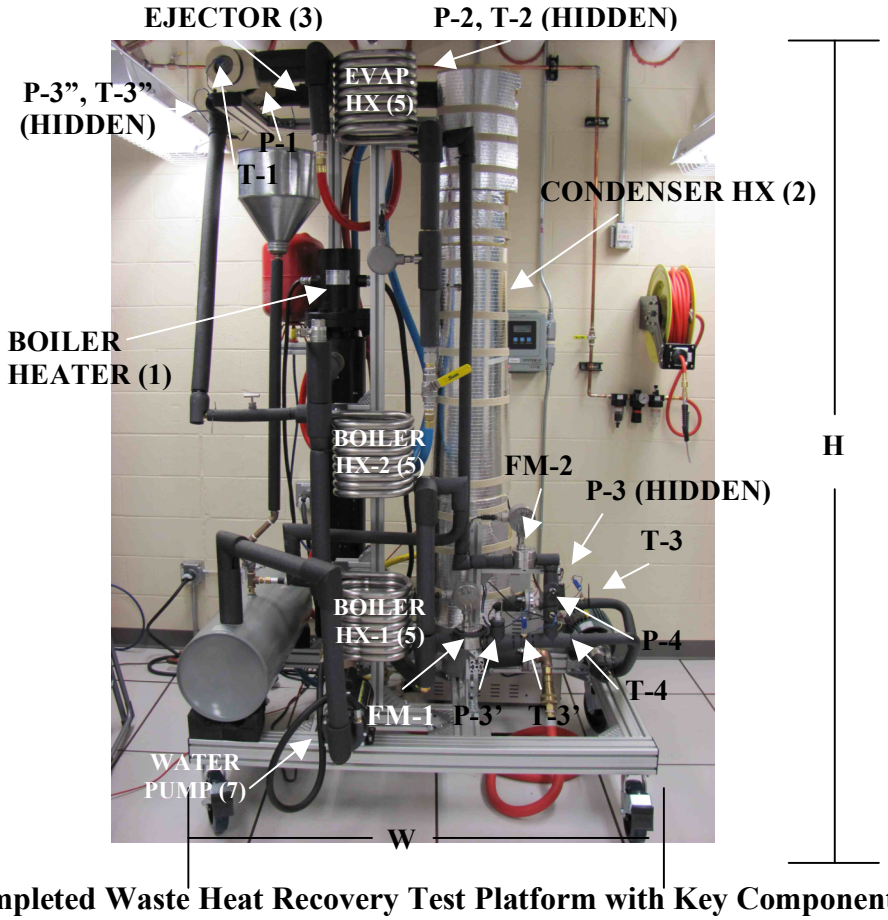

Figure 29. Completed Waste Heat Recovery Test Platform with Key Components Labeled
Overall Dimensions: H = 275 cm, W = 130 cm, D = 92 cm (into page)

Table 6. Key Component Capabilities and Manufacturers

Component	Designator	Dimensions in cm (LxWxH or LxD)	Capability	Manufacturer
Boiler Heater	1	100x20	40 kW Heater	Durex Industries
Condenser HX	2	200x15	43 kW	Yula Corporation
Ejector	3	28x5	Varies with port pressures	
Evaporator Heater	4 (Behind Structure)	76x30x45	PID controlled temperature, 3 kW heater	Sterling
Evaporator and Boiler HX	5	30x20x40	3-20 kW based on flow rate	Exergy, LLC
Refrig. Pump	6	45x25	VFD controlled flow, 550 kPa constant head	Tuthill Pumps
Water Pump	7	30x8		
Flow Meter	FM-#	10x10	± 0.5% FS	Omega Engineering
Pressure Transducer	P-#	5x2	± 0.5% of Measured	Omega Engineering
Thermocouple	T-#	7.6 cm Probe	± 0.2°C	Omega Engineering

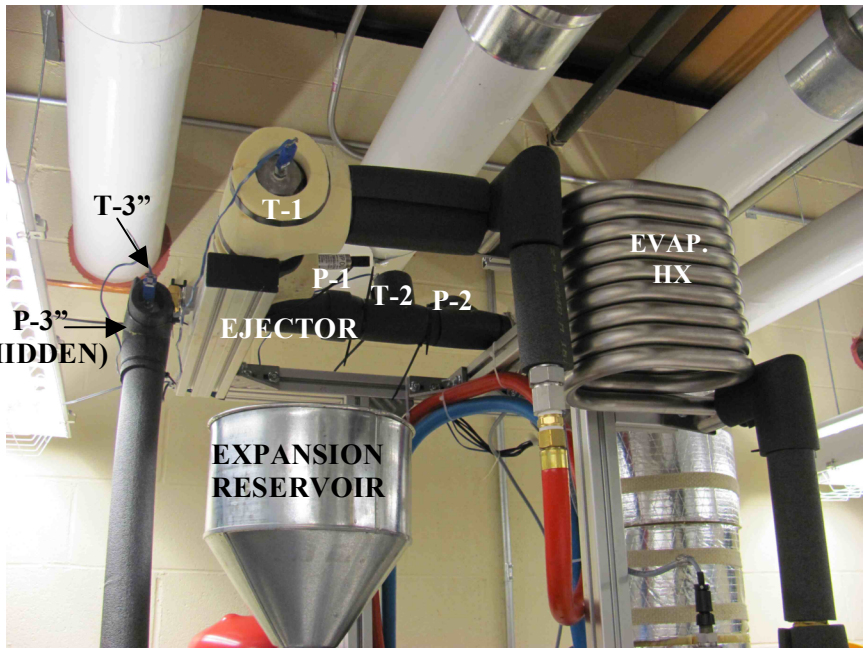

Figure 30. System Ejector Section with Local Components Marked

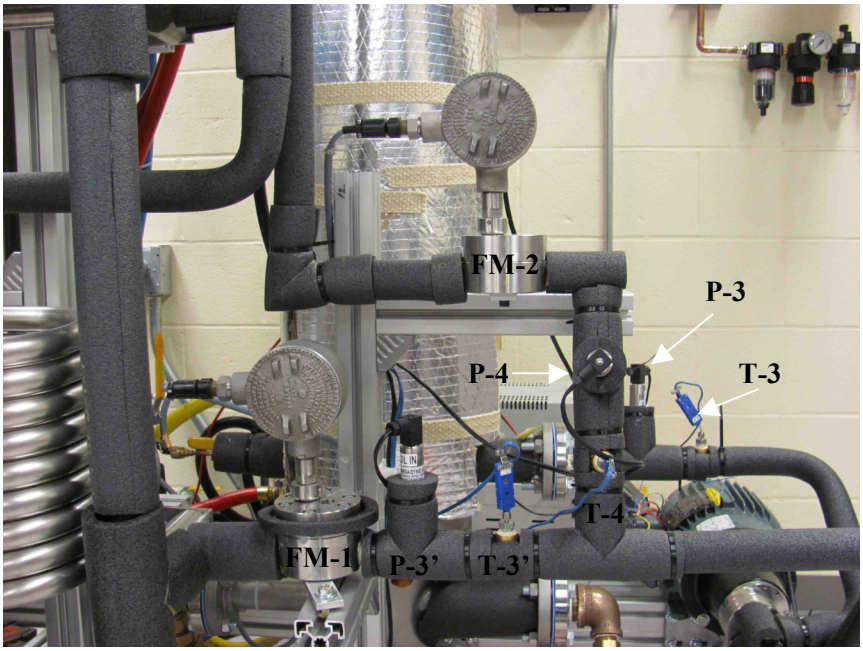

Figure 31. Refrigerant Flow Meters (FM-1 for Boiler flow, FM-2 for Evaporator Flow)

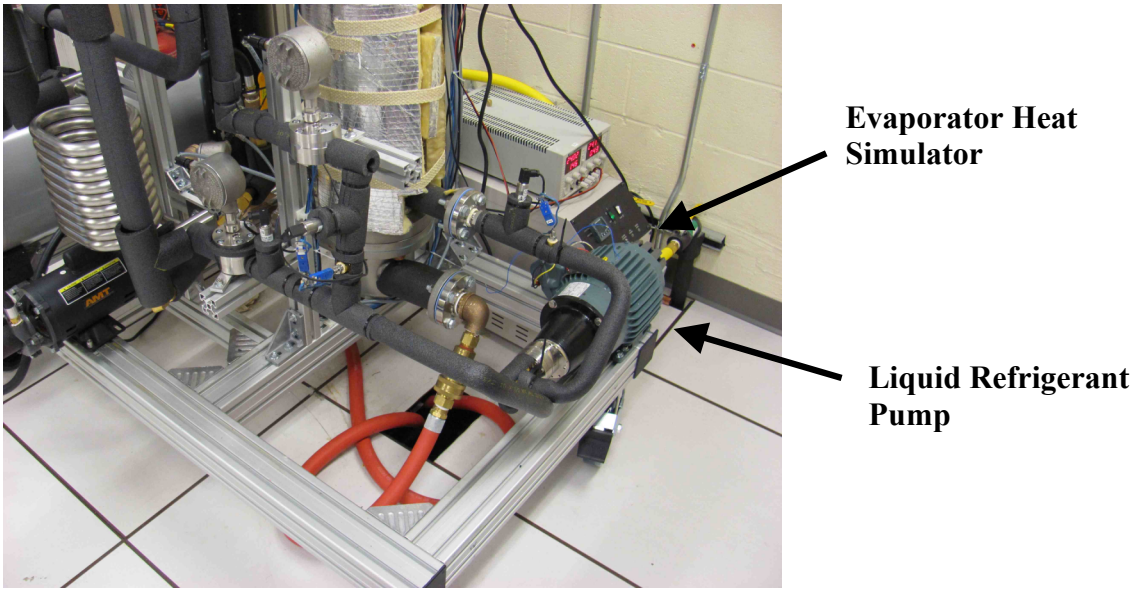

Figure 32. Refrigerant Pump Section with Evaporator Heater Visible

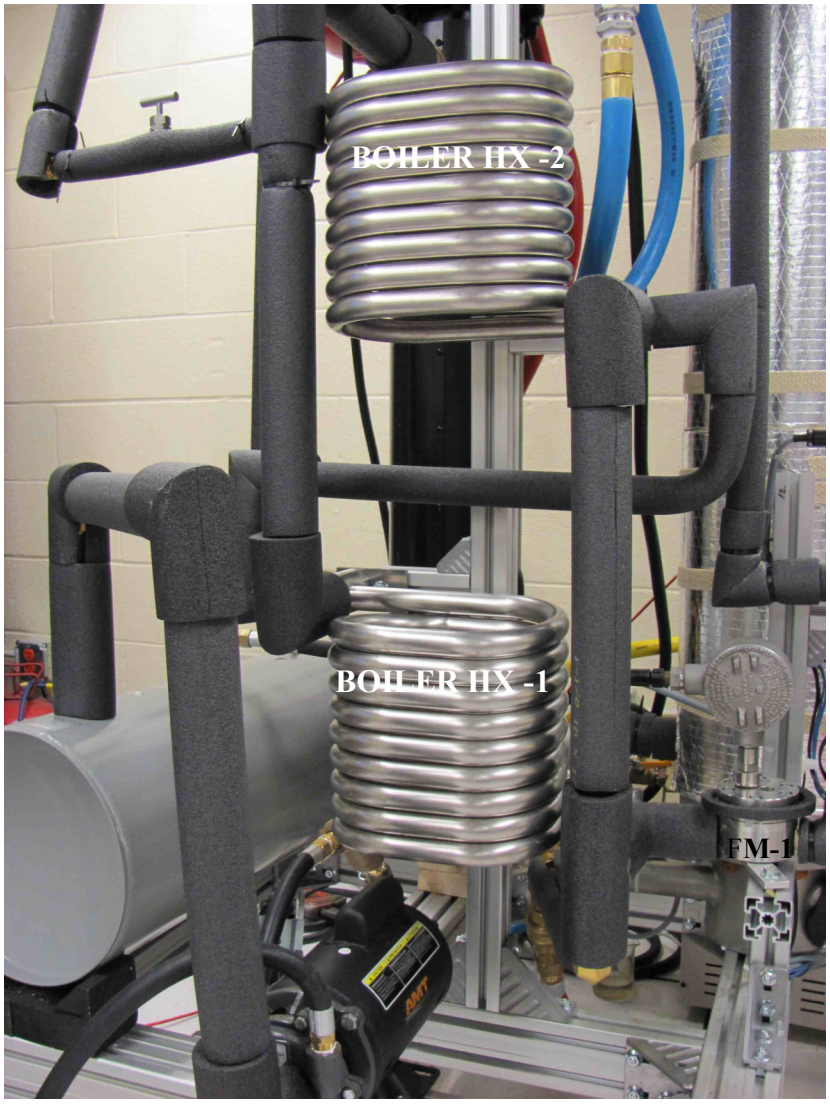

Figure 33. Boiler Water-to-Refrigerant Heat Exchangers (Boiler Water Pump Visible below Boiler HX-1)

3.2 Experimental Preparation

The thermocouple probes and pressure transducers were inserted into their respective places in the system and the refrigerant charging process began. The system was then pressurized with compressed air and pressure data was collected for 24 hours to verify a leak tight condition. The system was then evacuated via vacuum pump to a vacuum of 0.5 inches of mercury. Refrigerant was then added to the system through the refrigerant charging port, shown at the bottom of the refrigerant condenser in Figure 34.

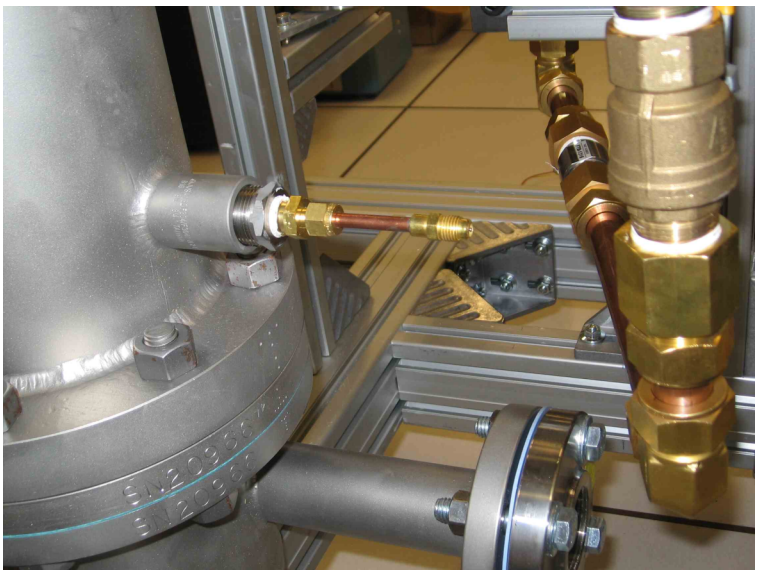

REFRIGERANT CHARGING PORT WITH VALVE

Figure 34. Refrigerant Charging Port with Built in Shrader Valve (Located at Bottom of Condenser HX)

The amount of refrigerant needed to operate the system was calculated by summing the volume of refrigerant at the various phase conditions throughout the system. Since the phases are set throughout the system, the amount of refrigerant was approximated by the expected density and the volume of the vessels that contained the refrigerant at each phase condition. In this case, referring to the temperature and pressure conditions detailed in the model, the amount of refrigerant was calculated to be approximately 45 lbs. As a result, 60 lbs of refrigerant were acquired to ensure adequate refrigerant to account for approximation errors.

Using refrigerant hose, the refrigerant was gravity fed into the system by elevating the refrigerant canister. As the refrigerant was being fed into the system, the LabView program provided pressure and temperature values for the refrigerant exiting the condenser. Recalling that the refrigerant pump demands a liquid at its inlet, the temperature and pressure were monitored closely to ensure that this condition was met. Simultaneously, the coolant distribution unit was running at a water supply set point of 10 °C to ensure condensed refrigerant at the inlet of the pump.

3.3 Experimental Procedure

Each experiment was conducted utilizing a specific component startup order. The boiler and evaporator heaters were initialized and set at the desired operating temperatures for approximately 30 minutes in order to achieve steady state heated water temperatures. The condenser was also operated for approximately 30 minutes in order to obtain constant temperature cooling water. Then, after verifying that all instruments were reading appropriate values, the refrigerant pump was started at a VFD speed of 10 Hz. The VFD speed was slowly increased to the operating speed of 17 Hz over the course of approximately 30 minutes to allow for the system to stabilize between each speed adjustment. The LabView program was used to monitor the temperatures, pressures, and flow rates during the startup process.

After the startup was completed, the flow control valve for the boiler and the expansion valve were adjusted in order to optimize the performance of the system for the user set boiler and evaporator temperatures. The valves were adjusted based on the flow ratio between the boiler and evaporator. Referring to the flow ratio determined by the model, the valves were tweaked in order to achieve an evaporator to boiler flow ratio of 0.10. At the end of the experiment, the component shut-down order was refrigerant pump, boiler heater, and evaporator heater.

3.4 Experimental Results: Set 1

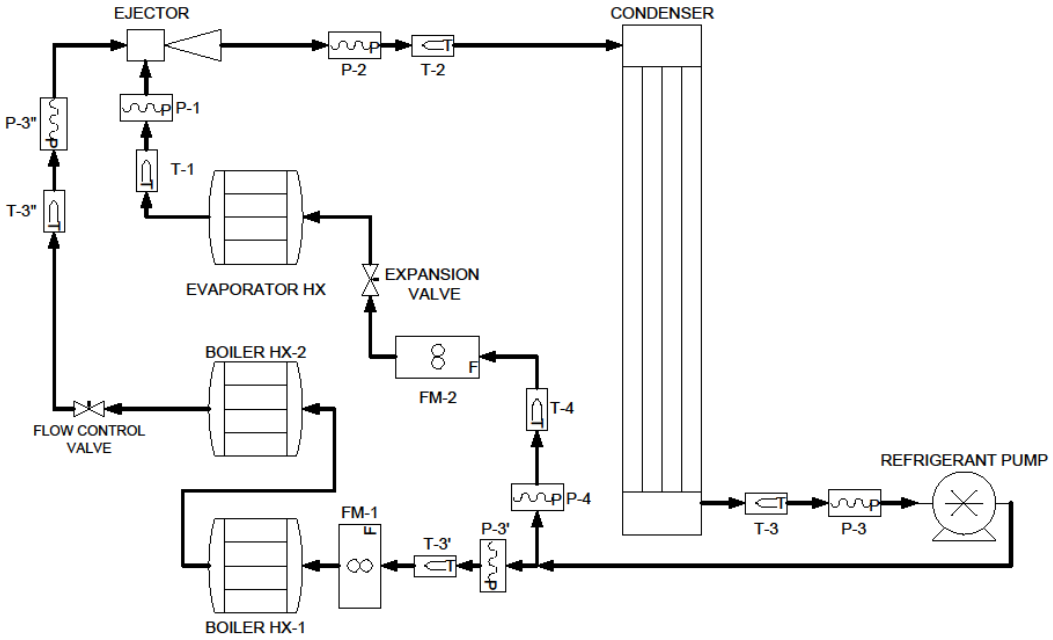

Figure 35: Experimental Schematic (For Key Component Details Refer to Tables 5 and 6)

Recalling the schematic for the experiment, the operating states for the experiments detailed in this section are outlined below in Table 7.

Table 7. System Parameters with Refrigerant Pump VFD Setting of 15 Hz [Set 1]

State	Temperature (°C)	Pressure (kPa)
1	23	112-113
2	62-70	117-119
3	12	116-118
4	13	116-118
3’	13	123-141
3”	70-80	123-141

The experiments were conducted over a period between 30 minutes and 2 hours, and were allowed to reach a steady state before shutting down the system. Figures 36 and 37 shows the temperature and pressure data, respectively. The spike located at approximately 400 seconds resulted from a temporary shut-down/start up of the refrigerant pump.

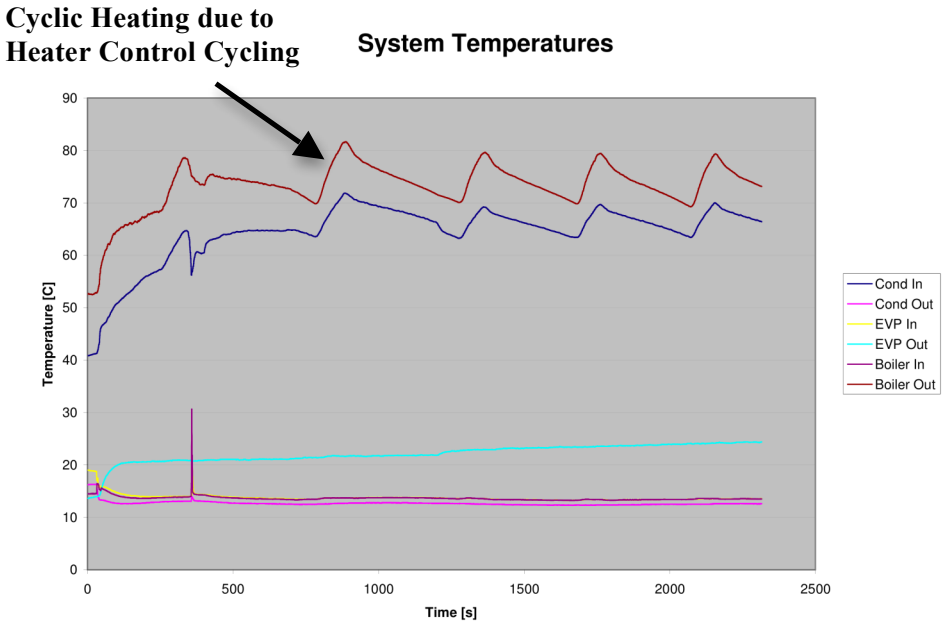

Figure 36. System Temperatures [Set 1]

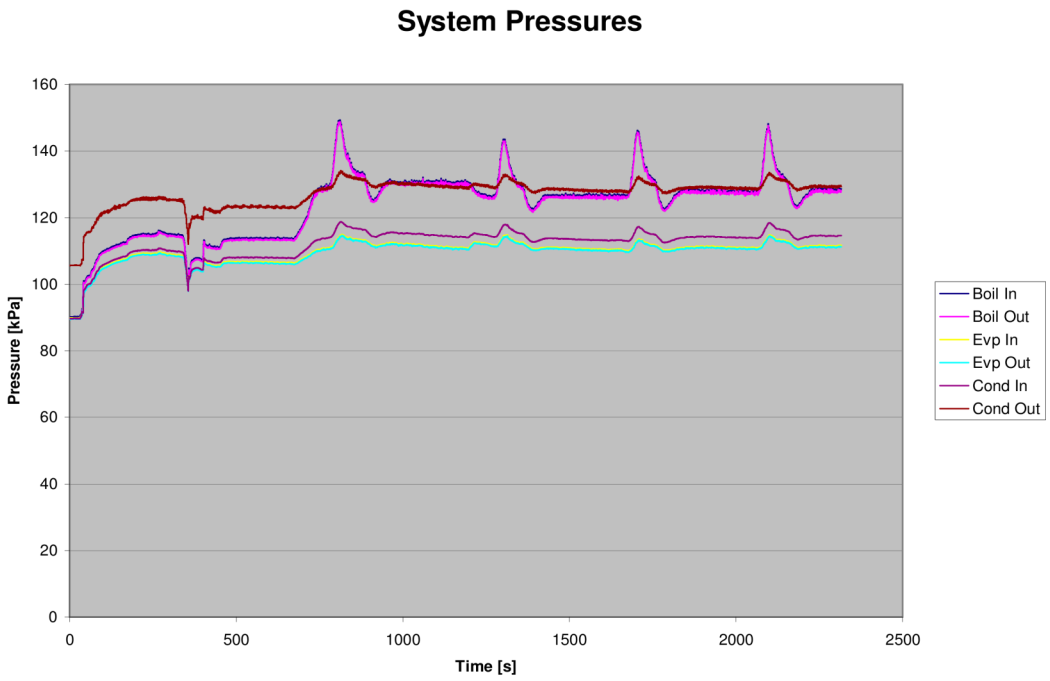

Figure 37. System Pressures [Set 1]

Due to unforeseen system pressure mixing, the boiler pressure was limited to a steady state value of approximately 130 kPa instead of the design point of 700 kPa. As a result, the model was altered to reflect the lower experimental pressures. The cyclic peaks seen in both the temperature and the pressure charts result from the unexpectedly crude temperature control thermostat used in the boiler heat simulator. The heater operated by using a bimetallic strip that would complete or break the heater circuit based on if the temperature was less than or greater than the value set by the operator. As a result, the heater exhibits a significant degree of temperature cycling, clearly visible in Figure 36, where the peaks correspond to the upper limit of the boiler heater temperature cycle and the troughs correspond to the lower limits of the boiler heater temperature cycle. During those moments, the refrigerant absorbs a greater amount of heat, which lowers the level of liquid refrigerant in the boiler heat exchanger. The temperatures and pressures settle when the refrigerant level in the boiler heat exchangers reaches their new steady state. A similar phenomenon is seen in the performance calculations as well.

Since the objective of these experiments is to determine the feasibility and performance of the ejector based refrigeration system, the system performance was calculated based on the boiler heat input and the evaporator heat input, as described in Equation 1. The results are shown in Figure 38.

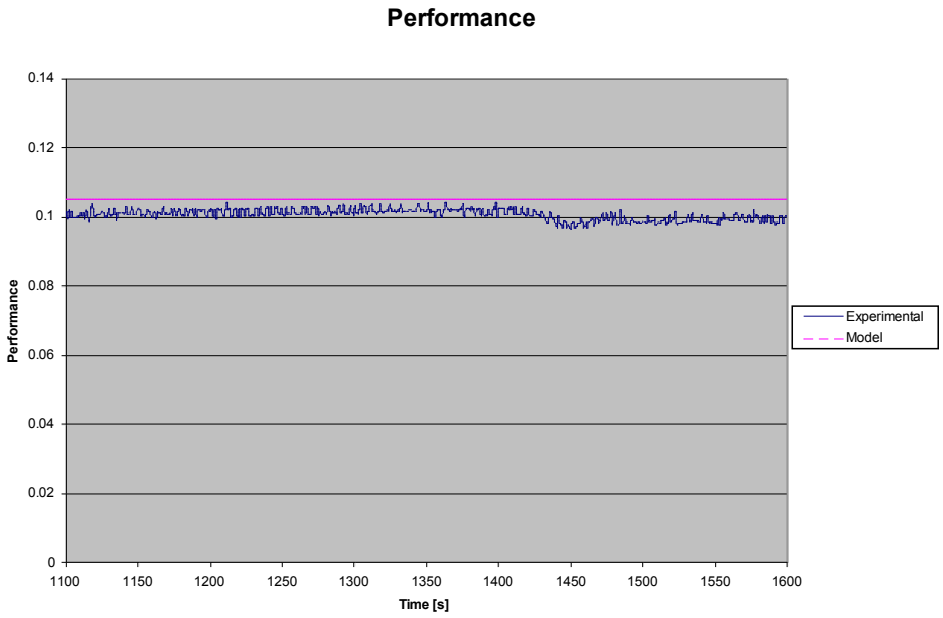

Figure 38. . Performance Chart using Experimental Data and Model using Experimental Temperatures and Pressures Observed for 1100<t<1600 [Set 1]

From this graph, the steady state performance between 1100 and 1600 seconds was calculated to be approximately 0.1, which agrees with the model predictions, represented by the dashed horizontal line. The entrainment ratio, and refrigeration effect, calculated by equation 5, also closely agree and are shown in Figures 39 and 40, respectively.

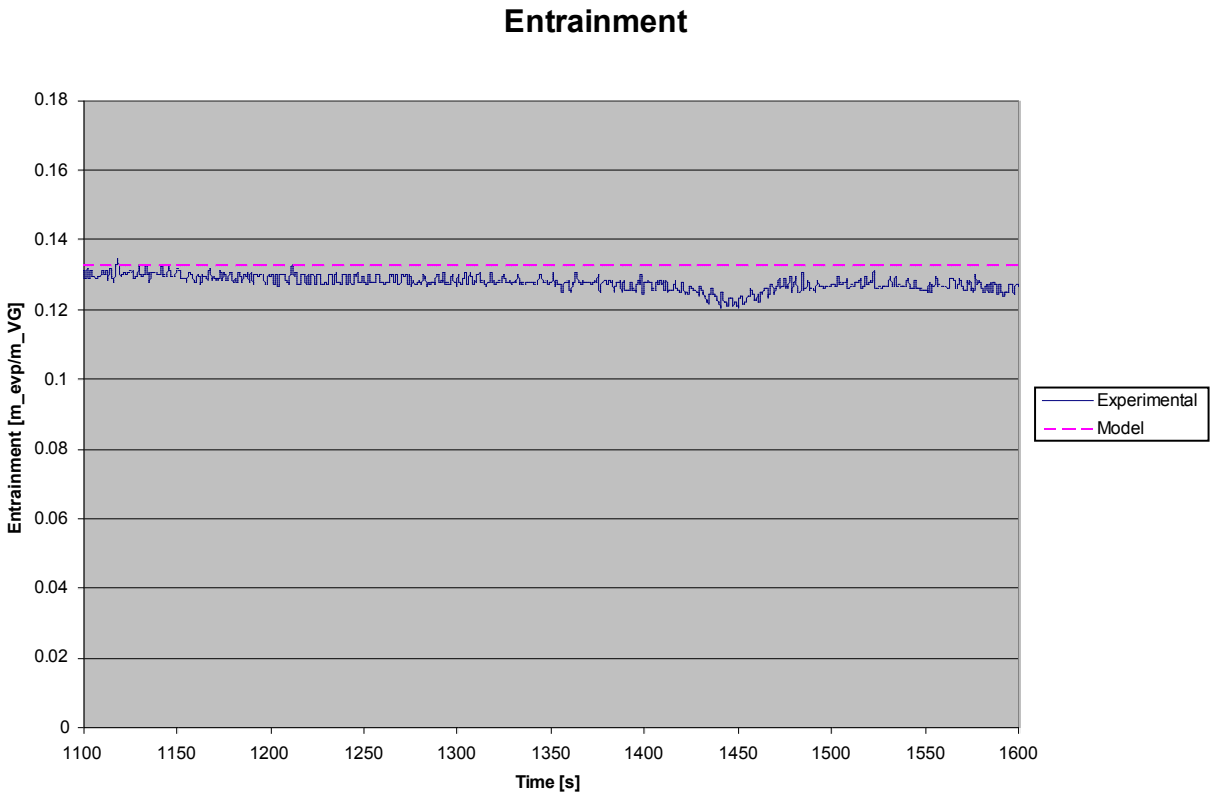

Figure 39. . Entrainment Ratio using Experimental Data and Model using Experimental Temperatures and Pressures Observed for 1100<t<1600 [Set 1]

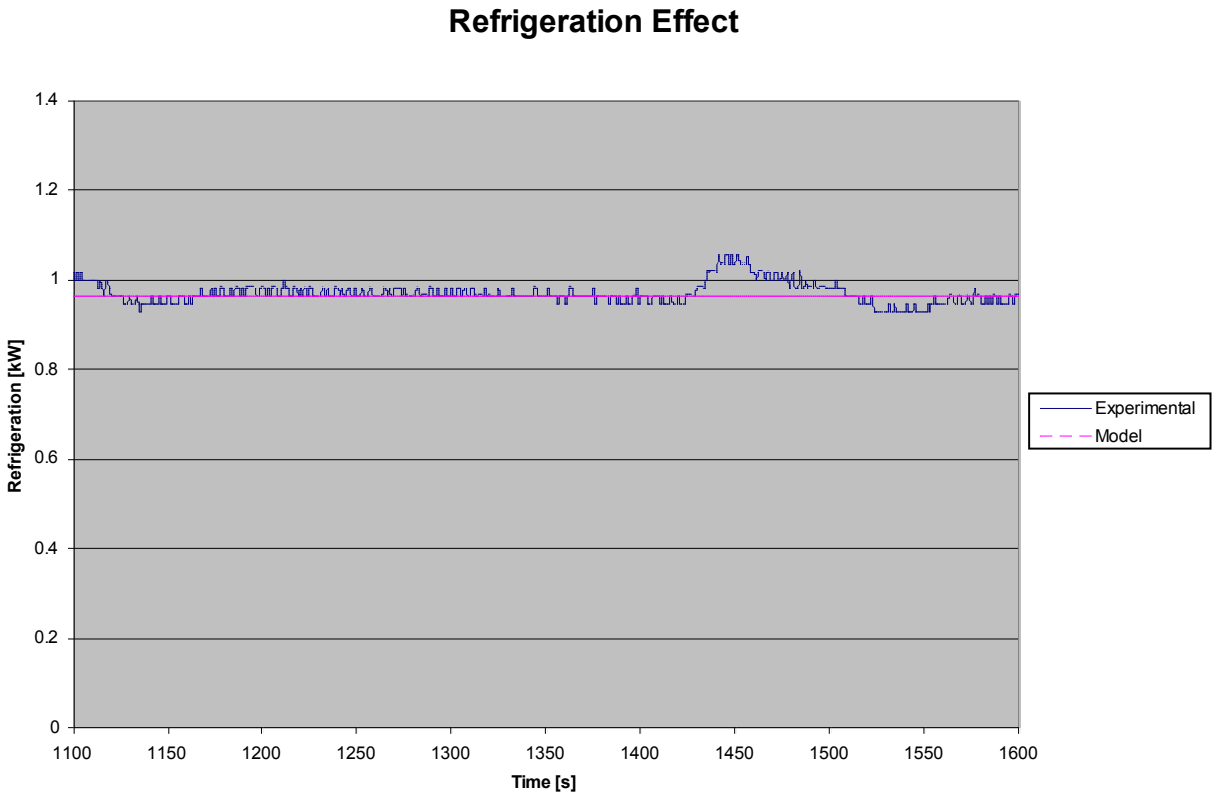

Figure 40. Refrigeration using Experimental Data and Model using Experimental Temperatures and Pressures Observed for 1100<t<1600 [Set 1]

The expected relationship between the performance and the entrainment ratio is clearly seen in Figures 39 and 40. The refrigeration effect is also affected by the entrainment ratio, but the temperature and pressure effects can also be seen in the periodic peaks. This is to be expected since the temperature and pressure values are used to determine the enthalpy at each data point and the enthalpy values are used to determine the heat loads in the evaporator and boiler.

Though the initial results held some promise, the nature of the system performance limitations (cyclic heating, flow rate cap) another set of experiments were conducted with a greater amount of refrigerant charge and a more refined PID heater controller. The PID controller uses temperature feedback from the system to cycle the boiler heater in order to

maintain a steady boiler temperature. The controller has an auto-tune function that allows the proportional, integral, and derivative multipliers to be set based on the system characteristics and response to the boiler heater input. The goal of the next set of experiments was to stabilize the heater fluctuations and increase the refrigerant flow rate to achieve the model prescribed refrigeration effect and ejector motive pressure. The results are reflected in sections 3.5 and 3.6

3.5 Experimental Results: Set 2

In the second set of experimental data, the refrigerant charge was increased to 21.75 kg (70 lbs), the PID heater controller was implemented. Table 8 shows the state parameters from the experimental set.

Table 8. System Parameters with Refrigerant Pump VFD Setting of 15 Hz [Set 2]

State	Temperature (°C)	Pressure (kPa)
1	24-26	140-145
2	48-78	142-148
3	11	160-170
4	11	140-145
3’	11	140-145
3”	73-80	148-160

The PID controller successfully stabilized the extreme fluctuations in temperature and pressure, but a new instability artifact arose due to the sensitivity of the system to the refrigerant flow control-valve positions. At about 9,000 seconds, the system was temporarily shut-off in order to slightly modify the refrigerant charge. The effects are shown in Figure 45.

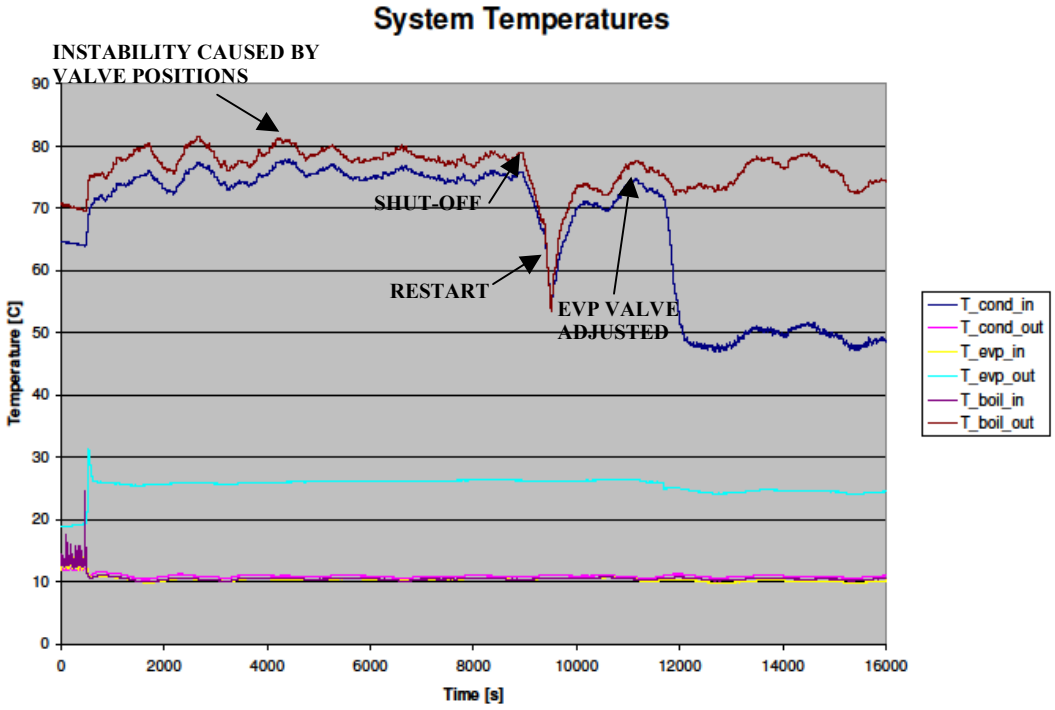

Figure 41. System Temperatures [Set 2]

The system pressures were not as effected by the valve imbalance, though some effects are still visible in the slight undulations present in the data.

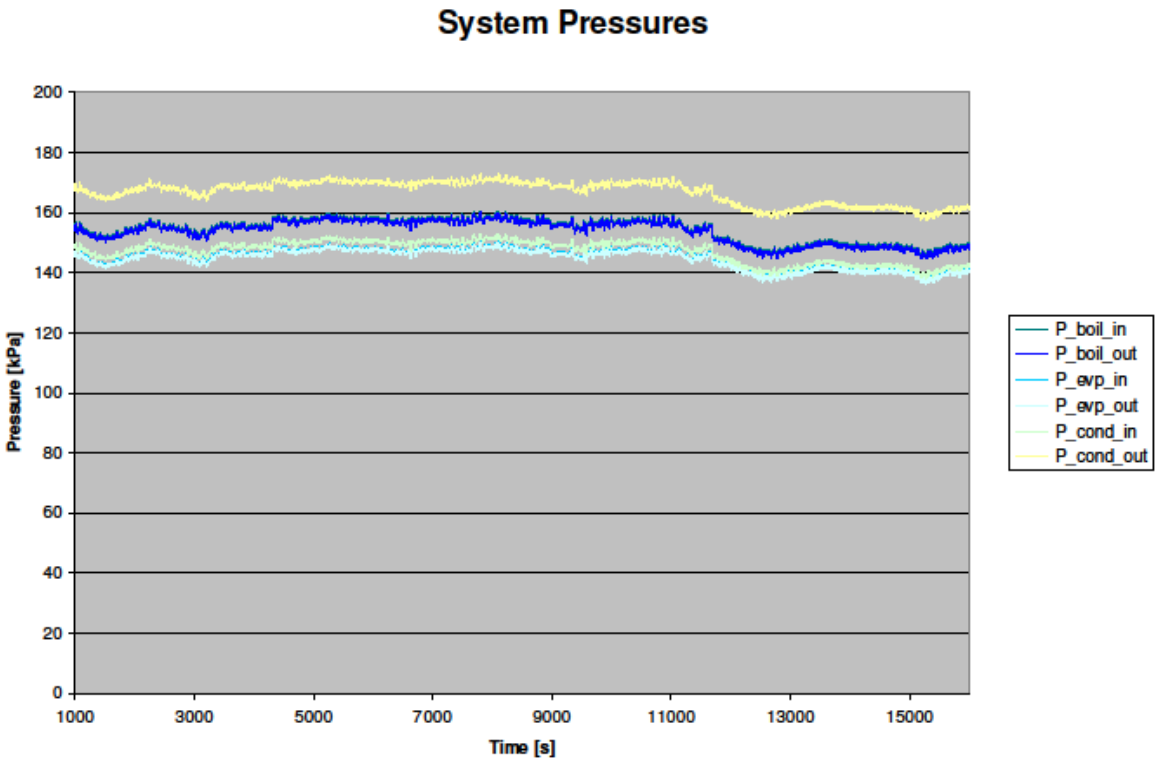

Figure 42. System Pressures [Set 2]

The performance graph of the second set of experiments brings to focus the extreme sensitivity of the system to the refrigerant flow rates and, thus, sensitivity to the refrigerant valve positions. After the expansion valve was tweaked, the performance of the system improved dramatically to approximately 0.06, which is comparable to the model predicted value of 0.062 when the experimental temperatures and pressures are used as the model input parameters. In addition, as expected, the entrainment ratio improved in a nearly identical manner, increasing from 0.025 to 0.07. This value agreed closely to the model predicted value of 0.083.

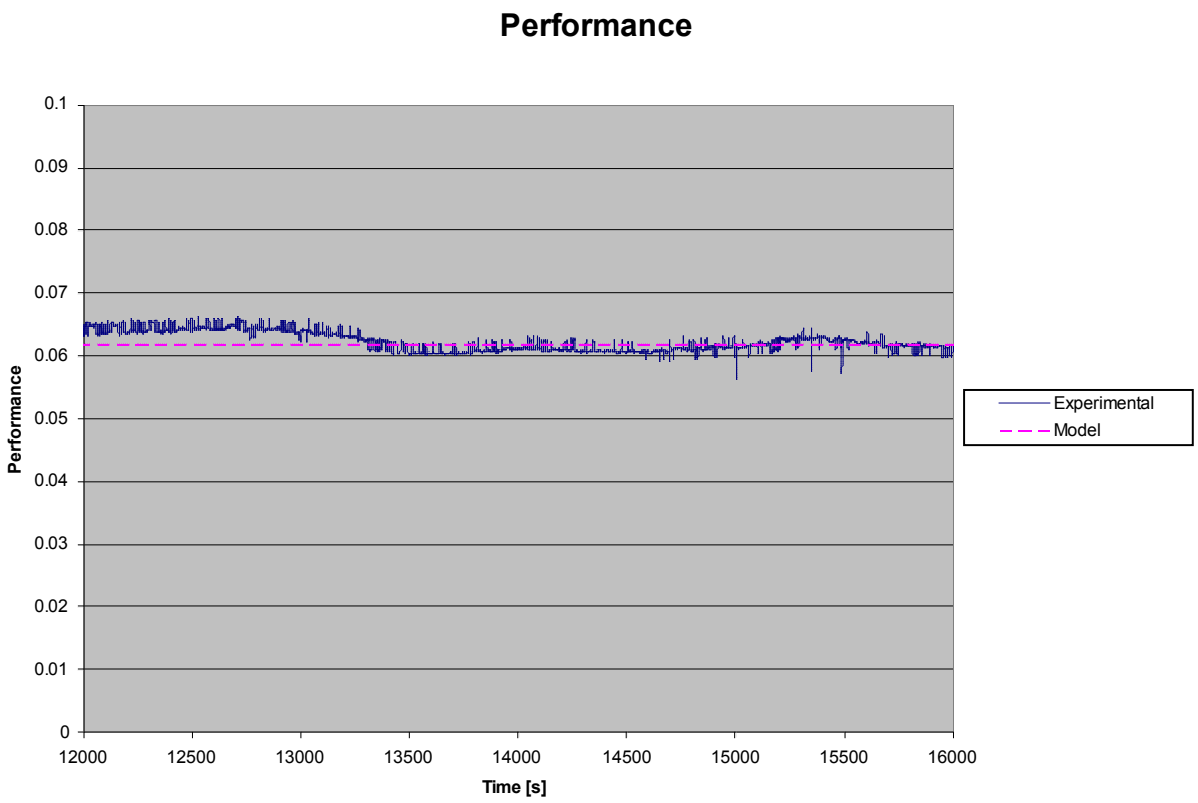

Figure 43. System Performance using Experimental Data and Model using Experimental Pressures and Temperatures Observed for 12000<t<16000 [Set 2]

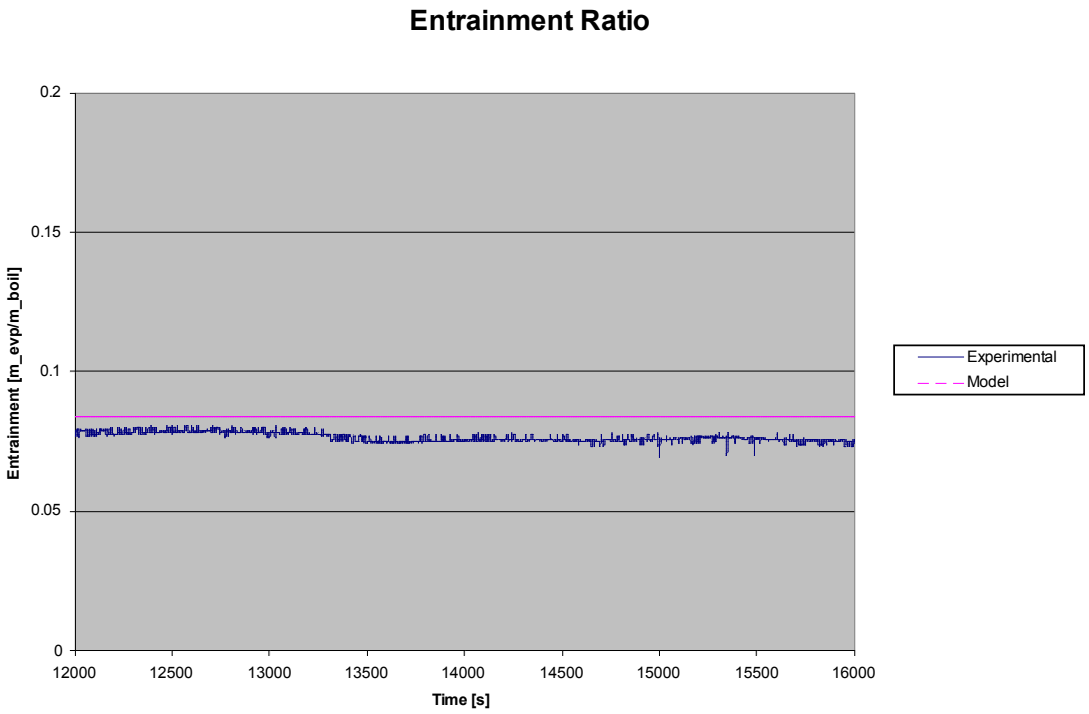

Figure 44. Entrainment Ratio using Experimental Data and Model using Experimental Pressures and Temperatures Observed for 12000<t<16000 [Set 2]

The final point of interest in the second set of experimental data is the refrigeration effect obtained. As Figure 45 shows, the refrigeration effect agreed closely to the predicted refrigeration effect for time 12000<t<16000.

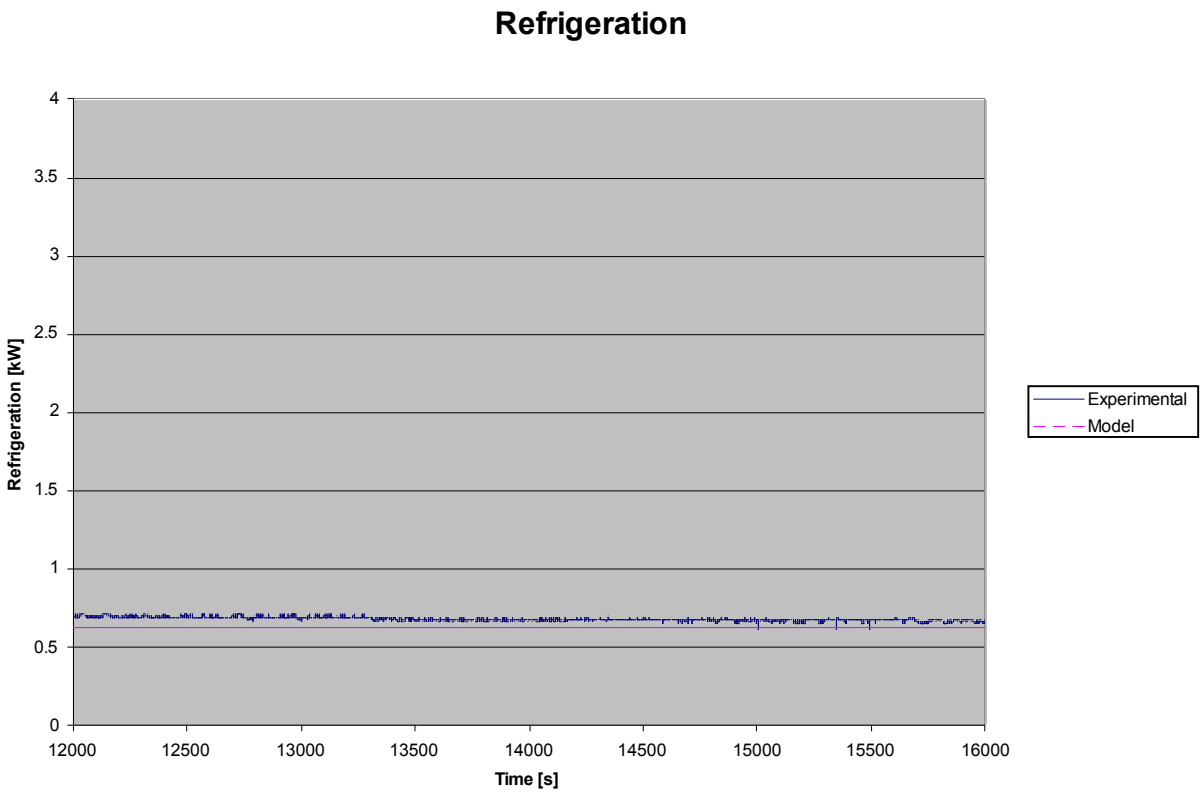

Figure 45. Refrigeration Effect using Experimental Data and Model using Experimental Pressures and Temperatures Observed for 12000<t<16000 [Set 2]

3.6 Experimental Results: Set 3

Table 9. System Parameters with Refrigerant Pump VFD Setting of 17 Hz [Set 3]

State	Temperature (°C)	Pressure (kPa)
1	25	140-145
2	56	142-148
3	11	160-170
4	11	140-145
3’	11	140-145
3”	73	148-160

The instability of the previous set of experimental results, as evidenced by the sporadic fluctuations in the pressure and temperature charts of the second experimental data set, is

eliminated by fine adjustments of the valve positions. The temperature control, as a result, improved and allowed for steadier operation. The temperatures were successfully maintained at or near the levels prescribed by the model, a condition that had previously been unattainable due to the periodic fluctuations and instability that have been eliminated in this experimental set.

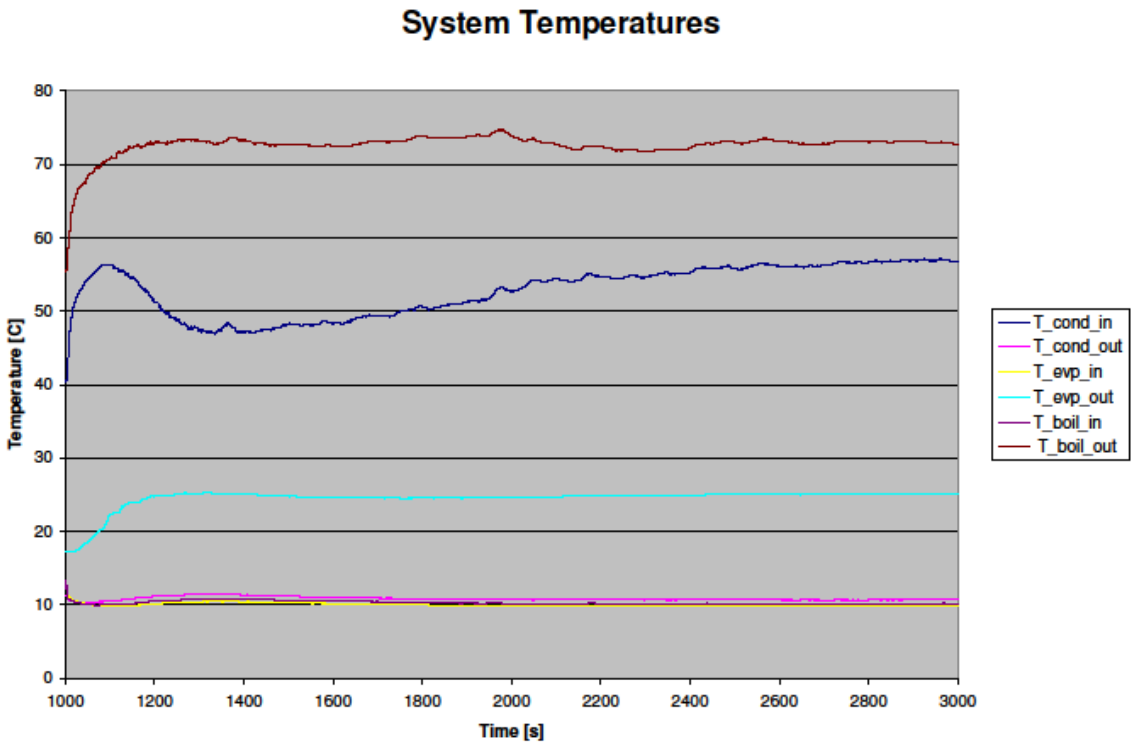

Figure 46. System Temperatures [Set 3]

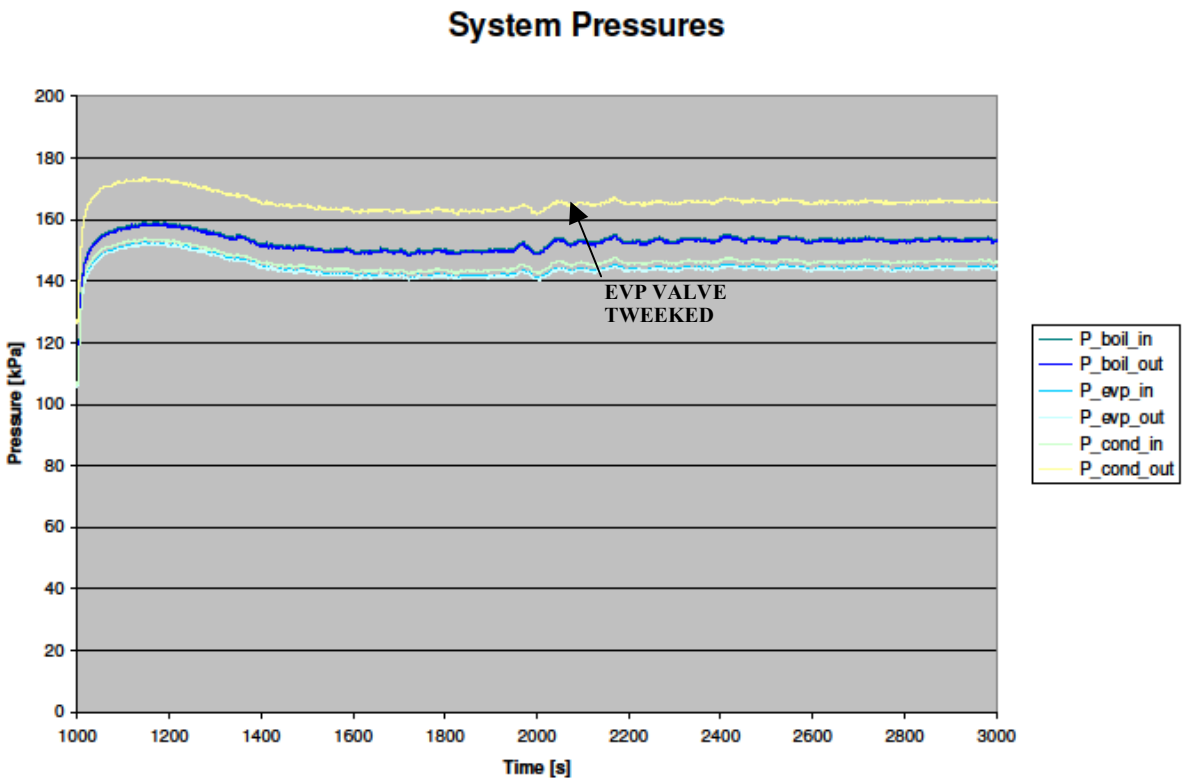

Figure 47. System Pressures [Set 3]

The performance, however, suffered slightly due to the slight modifications made to the valve positions. The stability was achieved at the expense of the performance. The same effect trickled down to the entrainment ratio and the refrigeration effect, which are all closely related through the refrigerant flow rate through the evaporator.

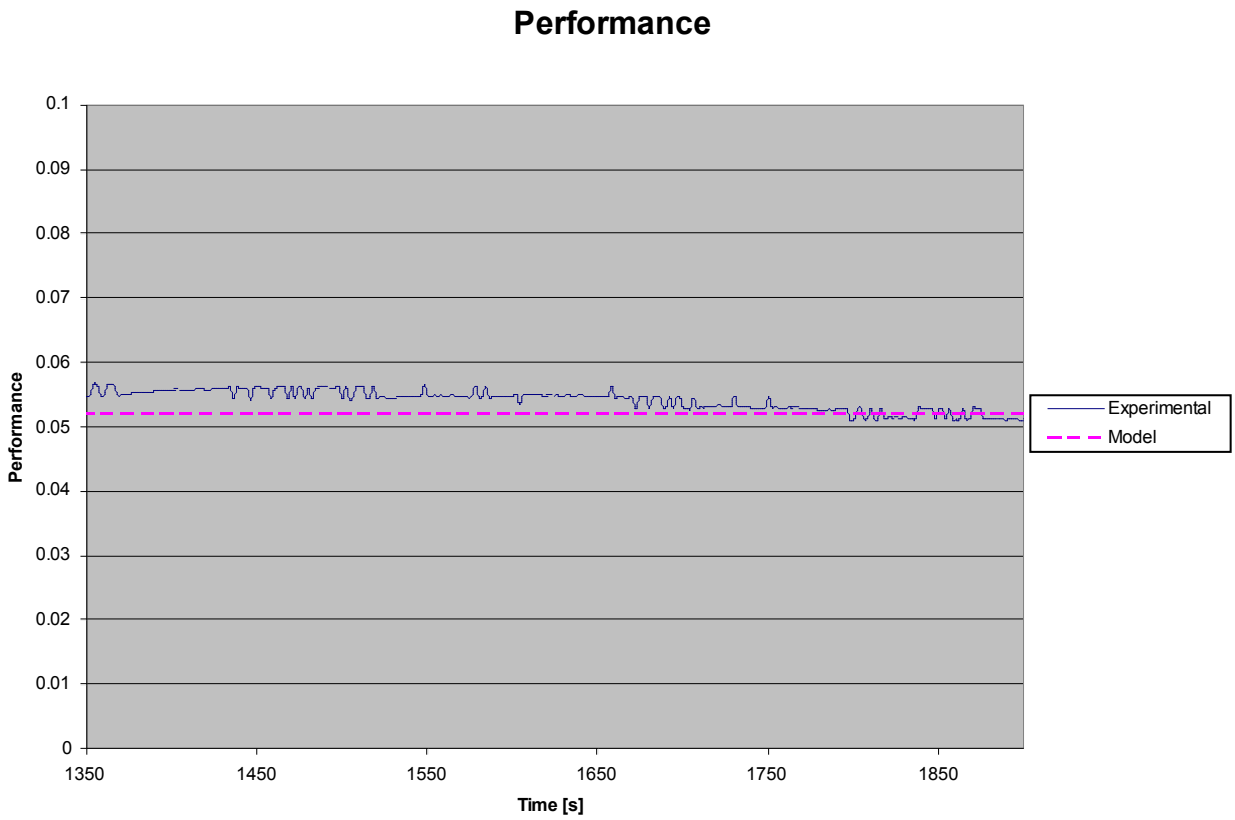

Figure 48. System Performance using Experimental Data and Model using Experimental Pressures and Temperatures Observed for 1350<t<1900 [Set 3]

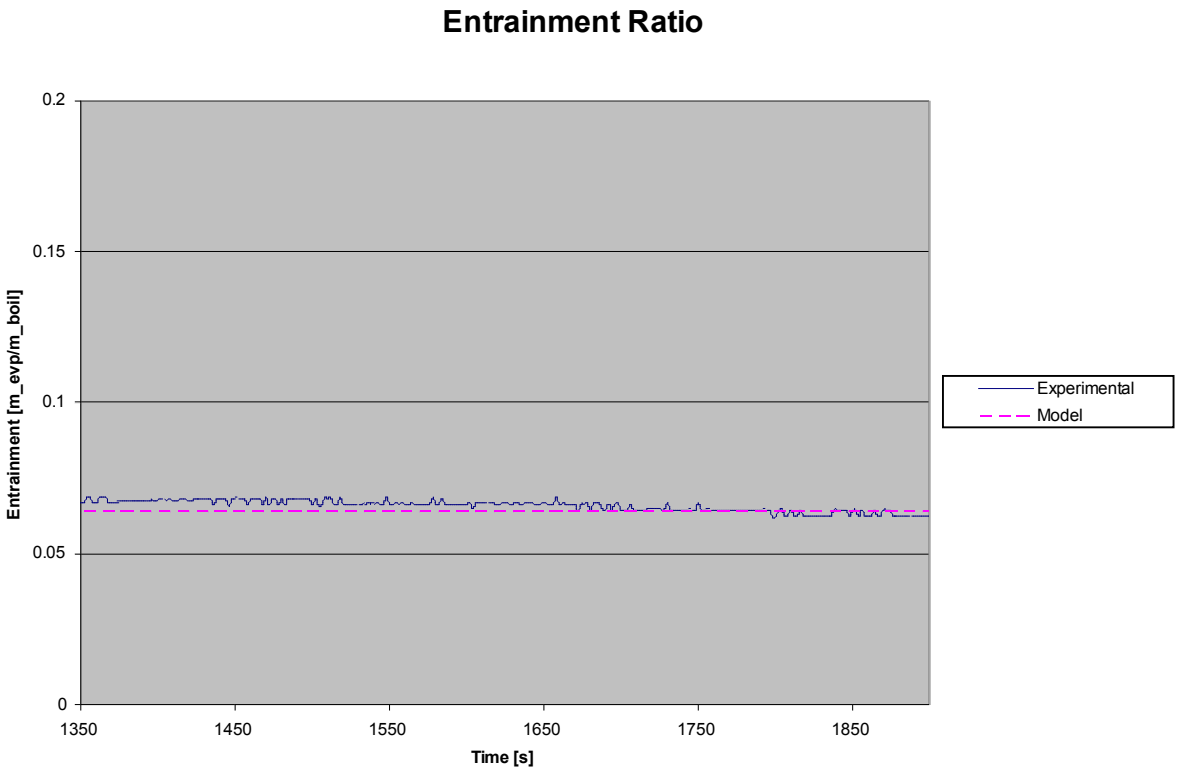

Figure 49. Entrainment Ratio using Experimental Data and Model using Experimental Pressures and Temperatures Observed During for 1350<t<1900 [Set 3]

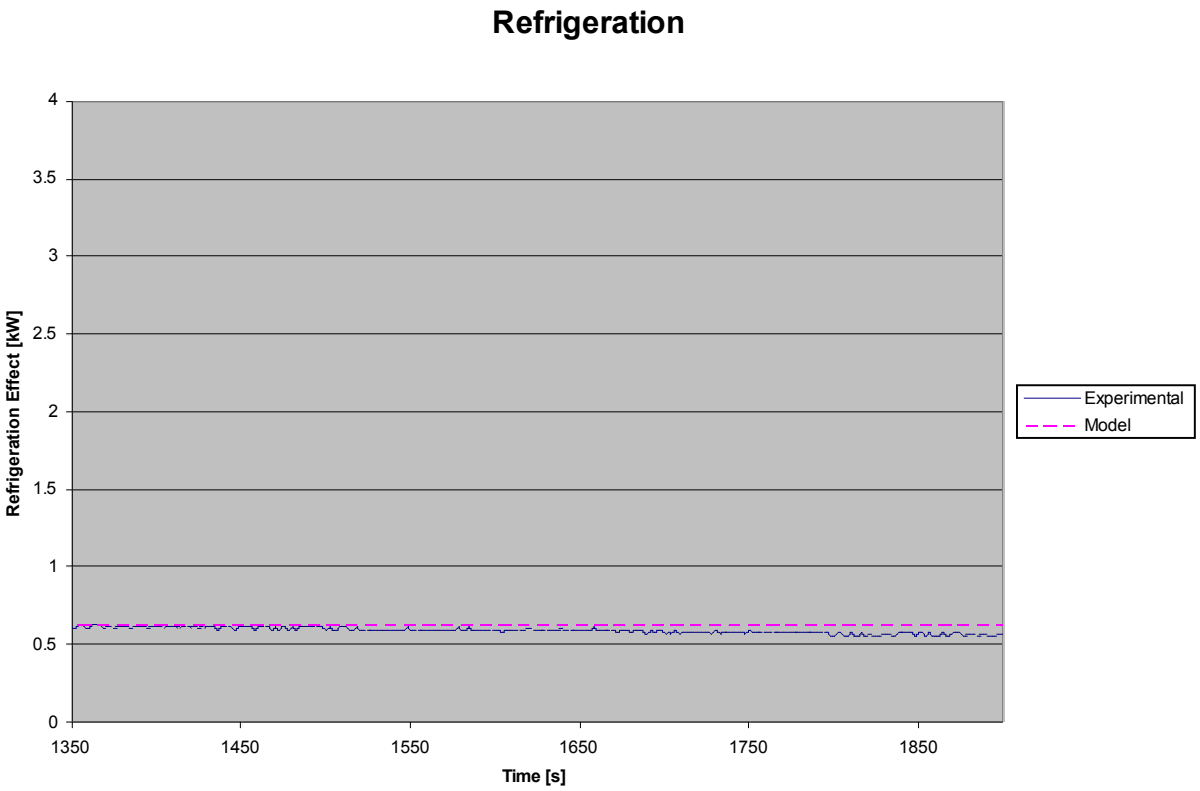

Figure 50. Refrigeration Effect Experimental Data and Model using Experimental Pressures and Temperatures Observed During for 1350<t<1900 [Set 3]

4. DISCUSSION

The common strands that run through all three sets of experiments are that the model closely approximates the characteristics of the ejector refrigeration system, and the system is highly dynamic. For proper operation, the ejector refrigeration system must have differentiable 'zones' for the boiler, evaporator, and condenser sections. However, since the ejector connects all three zones, proper ejector operation is absolutely essential to zone differentiation. If proper differentiation is not achieved, the fluids in the system tend to mix and create a singular system state instead of the seven distinct states necessary for operation.

The first set of experimental results revealed the effects that quasi-steady parameters can have on the stability and performance of the ejector refrigeration system. Even though the performance metrics suggested performance that was comparable to the predictions made by the model, the surges in temperature affects the instantaneous rate of refrigerant flow, which invites the possibility that the liquid refrigerant pump will be temporarily deprived of a steady refrigerant supply, potentially damaging the pump.

A cursory glance of the initial model predictions (detailed in Chapter 2) and experimental results reveals a dramatic discrepancy between the model temperature and pressure parameters and the experimental temperature and pressure parameters. The model was altered to reflect the operating parameters observed in the experimental data and the figures generated by the modified model used average temperatures and pressures over the specified time frame, *t*. The figures showed close agreement between the experimental data and the model, which seems to indicate that the model could also accurately predict the performance of the system at the original model operating conditions that were described in Section 2 of this thesis.

In order to avoid the potential of starving the refrigerant pump, a refined PID controller was installed to reduce the periodic heater control hysteresis that was causing the large fluctuations in fluid temperature, pressure, and flow rate. Additionally, refrigerant was added to the system to increase the liquid refrigerant buffer in case an unexpected surge in temperature temporarily altered the refrigerant flow rate. However, the second set of experiments introduced the internal instability of the system. The interaction between the three system 'zones' became evident in the data, as well as the effect that minute valve adjustments can have on the system performance. Careful and precise valve adjustments eventually led to the elimination of the effects of the instability in the third set of experimental results. Performance, however, was markedly reduced by the small adjustment.

Comparing the results in this thesis to results from the previous work described in Chapter 1, the operating parameters (temperature and pressures) of this thesis are most closely aligned with those from Khalil, et al. The maximum performance achieved in this thesis was approximately 0.12 using R245fa, whereas the maximum performance achieved by Khalil, et al. was 0.17 at a boiler temperature of 76°C. Most of the prior literature concludes that higher boiler temperatures (>85°C) lead to higher performance, as well as opens up the possibility of using many available working fluids. Future computing servers could conceivably provide higher temperatures, but current operating parameters dictate a lower boiler temperature, which severely reduces the maximum attainable performance and the options for a suitable working fluid.

5. FEASIBILITY REPORT

The system that was built to evaluate the feasibility of the waste heat driven ejector based refrigeration cycle revealed key strengths and weaknesses of the waste heat ejector recovery system concept. The performance metrics of the system were acceptable for waste heat applications, even though the operating conditions were far lower than the ejector's designed operating conditions. The stability of the system, however, varied greatly due to internal system dynamics. Adding the natural dynamics of the data center environment at the computing rack level would magnify the stability control issues observed in the experimental results of this thesis.

5.1 Scalability

The main components that must be scaled are the ejector and the refrigerant pump, both of which are available in a variety of sizes. Penberthy provides ejectors of comparable size to the ejector used in this thesis (25 cm in length and smaller), while Croll Reynolds provides custom designed and fabricated ejectors at sizes much larger than 25 cm in length [22]. Large refrigerant pumps are available through various companies, including Magnatex Pumps [23].

5.2 Broad Cost Analysis

In the system built in this thesis, the off-the-shelf ejector cost $365 (USD), and the refrigerant pump cost $3,950 (USD). Based on the experimentally determined performance of 10% , the achieved boiler heat load of approximately 9 kW, and assuming the cost of energy to be $0.11/kWh, the payback period for these two components would be approximately 4.5 years at a data center operating 18 hours a day [24]. Analysis of a hypothetical 1 MW data center facility with the same 10% waste heat recovery and energy cost operating at 50% capacity would

save approximately $361,000 in cooling costs each year. In this analysis, the refrigerant pump work was accounted for in the performance calculation.

5.3 Recommendations

Considering the economy of scale that could be achieved by consolidating the critical ejector system components (ejector, refrigerant pump), it is the opinion of the author that the ejector based waste heat recovery concept should be applied to 14 racks (unit cell) or more in order to benefit from centralizing the main components and reduce the ejector system heat input fluctuations. Also, centralization provides the added benefit of the choice of removing the ejector system components from the data center floor, leaving more space for additional servers.

6. CONCLUSIONS AND FUTURE WORK

The performance metrics calculated from the experimental data in this thesis closely followed the performance metrics predicted from the model. Difficulty in realizing zone differentiation led to blending of zone pressures, which reduced the expected pressure potential between the boiler and evaporator to around 50 kPa from around 600 kPa. The compression observed in the experiments reflects the dramatic reduction in pressure potential.

In a future rack deployable system, dynamic server loading could introduce control/optimization issues. Intentional, dynamically controlled load migration could reduce the dynamic server effects by supplying steadier input parameters to a rack deployed ejector refrigeration system. Also, a more refined expansion device control method could improve real-time refrigerant flow adjustment to allow for some adaptation to the dynamic data center environment. Additionally, applying the ejector system to the facility level could reduce the dynamic effect of the data center by reducing the variability in instantaneous heat load

Finally, since each data center environment is different, the geometrical constraints of the ejector necessitate custom ejector construction for each unique set of input parameters. It is possible to fabricate an ejector with variable geometries, however, a very complex and complete control algorithm must accompany such an ejector design to ensure proper operation.

INDIVIDUAL CONTRIBUTIONS

This thesis applies an existing system to a new field with different operating conditions. This thesis describes an application of ejector based waste heat recovery to lower temperatures of approximately 75°C. A small scale simulation platform was designed and constructed to assess the operation of the ejector system using data center heat loads and temperatures. Additionally, a waste heat recovery refrigerant was found that operates well at data center conditions, and was subsequently explored and incorporated successfully into the ejector system.

This thesis reflects a first-stage examination of the ejector based waste heat recovery refrigeration system applied to data centers. To the knowledge of the author, no other experimental work has attempted to explore the feasibility of an ejector system for the temperature and heat load characteristics of a data center.

APPENDIX

Uncertainty Analysis

Necessary in any serious field of research that utilizes sophisticated instrumentation, uncertainty analysis aids in the dissection of useful data, as well as the identification of possible design weaknesses. The uncertainty analysis employed in this thesis employs the methods described by Moffat [25]. The three instruments that contributed to the uncertainty of the ejector refrigeration system are the pressure transducers, thermocouples, and the flow meters. For clarity in the graphical representation, a subset was taken from the raw data by applying a filter that only selected a set number of values, equally spaced in time, that gave a fair representation of the overall sample. The temperature and pressure subsets for one set of experimental data are represented in Figure A1 and Figure A2, respectively.

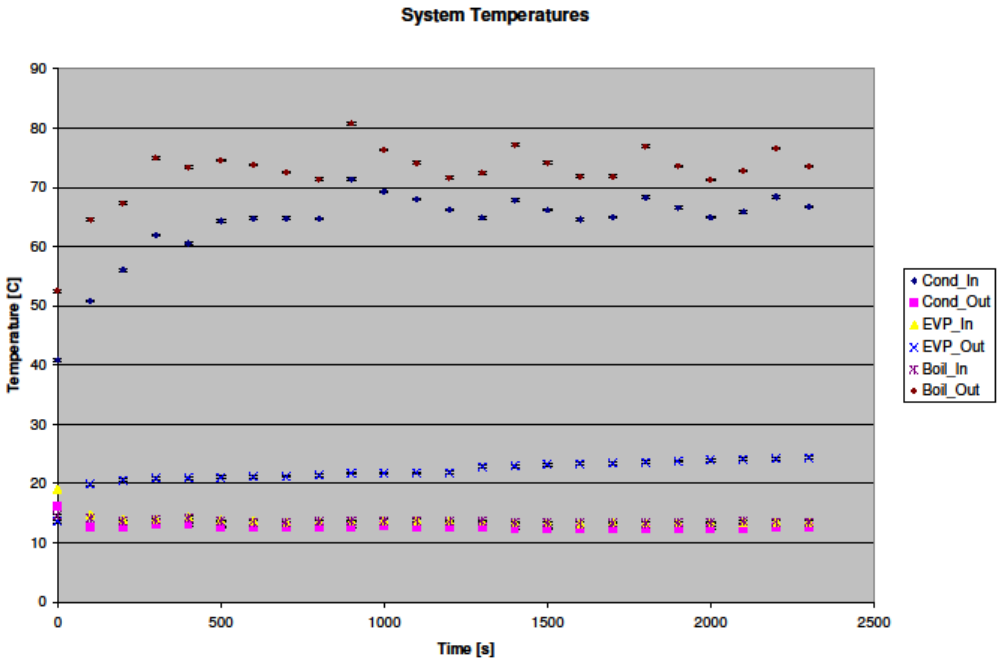

Figure A 1. Temperature Subset with Error Bars

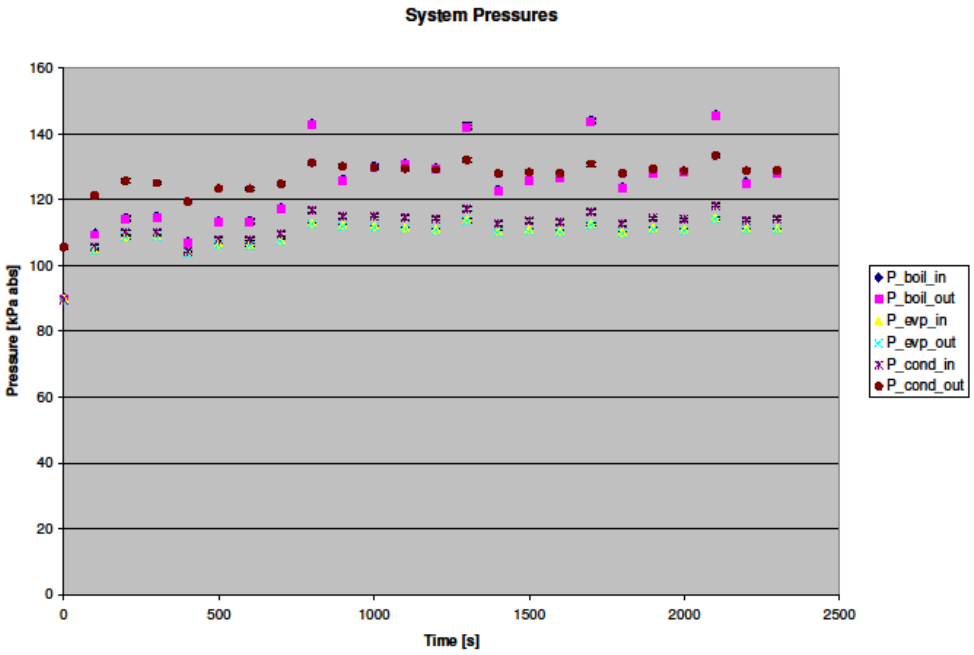

Figure A 2. Pressure Subset with Error Bars

The error represented in these figures is hard to distinguish due to the low level of uncertainty associated with these instruments. Also, the propagated error effects are almost indistinguishable for the performance metrics. For this reason, the uncertainty in the performance, refrigeration effect, and entrainment ratio are listed below in Table A1.

Table A 1. Maximum Uncertainty in Measurements

Measurement	Max Uncertainty	Units
Temperature	± 0.2	C
Pressure	± 1.5 kPa	kPa
Flow Rate	± 2.25	mL/min
Refrigeration	± 3	W
Entrainment	± 0.0001	[dim]
Performance	± 0.0005	[dim]

REFERENCES

[1] EPA, Report to Congress on Server and Data Center Energy Efficiency, in Energy Star Program. 2007.

[2] Garday, D., Air-Cooled High Performance Data Centers: Case Studies and Best Methods, D. Costello, Editor. 2006, Intel Information Technology.

[3] Patterson, M.K. and D. Fenwick, The State of Data Center Cooling: A Review of Current Air and Liquid Cooling Solutions. 2008.

[4] (2008) Data Center Energy Forecast.

[5] Novotny, S., Green Field Data Center Design - Water Cooling for Maximum Efficiency. 2010, Vette Corporation.

[6] CoolCentric, LiquidCool Rear Door Heat Exchanger. 2010.

[7] Roger Schmidt, M.E., Madhu Iyengar, Gary New. IBM's Power6 High Performance Water Cluster at NCAR - Infrastructure Design-. in IPACK2009. 2009. San Francisco, California, USA.

[8] Fournier, E., Using Thermal Energy Storage for Data Center Cooling, The Fortress International Group.

[9] Bianchi, M., and A. De Pascale. "Bottoming Cycles for Electric Energy Generation: Parametric Investigation of Available and Innovative Solutions for the Exploitation of Low and Medium Temperature Heat Sources." Applied Energy 88 (2011): 1500-509. Print.

[10] Gould, C. A., N.Y.A Shammas, S. Grainger, and I. Taylor. "Thermoelectric Cooling of Microelectronic Circuits and Waste Heat Electrical Power Generation in a Desktop Personal Computer." Material Science and Engineering B 176 (2011): 316-25. Print.

[11] Radchenko, A., Assessment of Ejector Waste Heat Refrigeration for Pre-Cooling Gas

Turbine Inlet Air, in International Symposium on Heat Transfer in Gas Turbine Systems. 2009: Antalya, Turkey.

[12] Khalil, A., et al., Ejector design and theoretical study of R134a ejector refrigeration cycle, International Journal of Refrigeration (2011), doi:10.1016/j.ijrefrig.2011.01.005

[13] ASHRAE, Steam-Jet Refrigeration Equipment. Equipment Handbook. 1983.

[14] Yapici, R., H. K. Ersoy, A. Aktoprakog˘lu, H. S. Halkacı, and O. Yig˘ It. "Experimental Determination of the Optimal Performance of Ejector Refrigeration System Depending on Ejector Area Ratio." International Journal of Refrigeration (2008): 1183-1189.

[15] Boumaraf, L., and A. Lallemand. "Modeling of an Ejector Refrigerating System Operating in Dimensioning and Off-dimensioning Conditions with the Working Fluids R142b and R600a." Applied Thermal Engineering 29.2-3 (2009): 265-74. Print.

[16] Chunnanond, K., and S. Aphornratana. "An Experimental Investigation of a Steam Ejector Refrigerator: the Analysis of the Pressure Profile along the Ejector." Applied Thermal Engineering 24.2-3 (2004): 311-22. Print.

[17] Yapici, R., and H. Ersoy. "Performance Characteristics of the Ejector Refrigeration System Based on the Constant Area Ejector Flow Model." Energy Conversion and Management 46.18-19 (2005): 3117-135.

[18] Meyer, A., T. Harms, and R. Dobson. "Steam Jet Ejector Cooling Powered by Waste or Solar Heat." Renewable Energy 34.1 (2009): 297-306. Print.

[19] Decoufle, B., Raise the Temperature Limit for Data Center Equipment and Help Save Cooling Costs. The Data Center Journal, 2007.

[20] I ncropera, Frank, David DeWitt, et. Al. Fundamentals of Heat and Mass Transfer 6th Edition.. Wiley. 2006.

[21] Penberthy of Tyco Valves and Controls, Ejector Manufacturer.

[22] Croll Reynolds of New Jersey, ejector manufacturer

[23] Magnatex Pumps, Magnetic Drive Pump Manufacturer.

[24] Average Energy Prices , United States Department of Labor.

[25] Moffat, R. J. "Describing the Uncertainties in Experimental Results." Experimental Thermal and Fluid Science. New York: Elsevier., 1988.

[26] 3M, Flourinert Electronic Liquid FC-72 Manufacturer.

[27] Dupont, Refrigerant HFC-134a Manufacturer.

[28] Durex Industries, Water Circulation Heater Manufacturer.

[29] Exergy, LLC, Compact Tube-in-Tube Heat Exchanger Manufacturer.

[30] Holman, J.P. Experimental Methods for Engineers, 7th edition. Boston: McGraw Hill, 2001.

[31] Honeywell, Refrigerant 245fa Manufacturer.

[32] Moran, Michael, and Howard Shapiro. Fundamentals of Engineering Thermodynamics, 5th Edition. Hoboken: Wiley, 2004.

[33] Sterling, Water Temperature Control Unit Manufacturer.

[34] Yula Corp, High Density Condenser Manufacturer.